

Reservoir Characterization of Kadanwari Gas Field Using Petrophysics and Seismic Inversion Integrated with Seismic Interpretation and Fault Seal Analysis



By

Bilal Ahmad Siddiqui
M.Phil (Geophysics)

Department of Earth Sciences
Quaid-i-Azam University
Islamabad

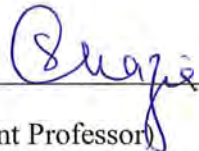
2015-2017




CERTIFICATE

It is certified that **Mr. BILAL AHMAD SIDDIQUI S/O ZIABAT KHAN** carried out the work contained in this dissertation under my supervision and accepted in its present form by Department of Earth Sciences as satisfying the requirements for the award of M. Phil degree in Geophysics.

RECOMMENDED BY:

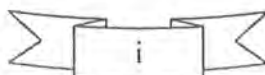
Dr. Shazia Asim 
(Supervisor/Assistant Professor)
(Department of Earth Sciences)

Dr. Mona Lisa 
(Chairman Department of Earth Sciences)

EXTERNAL EXAMINER: _____

**Department of Earth Sciences
Quaid-i-Azam University
Islamabad**

2015-2017



Dedication

I consecrate my work to my worthy parents and estimable teachers, whose prayers and efficacious devotion to my Studies encouraged me to achieve this Landmark.



Acknowledgement

I humbly obliged to the benevolent and merciful Allah for His uncounted and innumerable blessings throughout my life especially in the success of this project. The objective was unattainable without the prayers of my affectionate parents.

I owe a debt of sincere gratitude, jovial obligation and appreciation to my worthy teacher **Dr. Shazia Asim** and whole faculty of Earth Sciences Department for his guidance, insightful comments and valuable suggestions.

I want to pay my heartiest tribute to all friends for their consistent encouragement, cooperation, inspiring guidance in my project. They remained a generative force, a fountain-head and valuable assistance throughout.

Bilal Ahmad Siddiqui

QAU, Islamabad

ABSTRACT



This research work is done for reservoir characterization of Kadanwari gas field by using 2D and 3D seismic data along with well data of three wells Kadanwari-08, Kadanwari-10 and Kadanwari-16. It lies in middle Indus basin of Pakistan.

Based on well data four horizons are marked which are Upper Goru, Lower Goru, G Sand and E Sand. Then Time contour maps are generated to find the horizons trend and overall structure of this area. Then seismic velocities are used to change the time data to depth. Depth contour maps are generated to find the depth of these horizons and their thickness in study area. Seismic interpretation shows that in this area normal faults are present in the form of Horst and Graben.

Petrophysical analysis of two wells Kadanwari-08 and Kadanwari-10 is done to find out the reservoir zones and pay zone based on volume of shale, Porosity, resistivity, water saturation. Facies modeling is done to differentiate between the shale and sand lithology and to discriminate the gas sand from the Brine sand.

Fault seal analysis is used to find the sealing capability of faults which are present in the study area. First Juxtaposition diagram is used to check whether there is seal here due to juxtaposition of different lithologies. Then shale gouge ratio method is used to check that faults itself are acting as a seal or not. Seismic attribute analysis is done to confirm the seismic interpretation done previously. In this different attribute are used such as reflection strength, Phase and average energy.

Seismic inversion is used here to characterize the reservoir zone. First P impedance model is computed from the well data and interpretation data and then it is used for inversion to get the impedance section. On impedance section reservoir zone is picked by low value of impedance. This impedance model is used to find the porosity distribution of G sand in the 3D seismic area. This porosity is compared with the petrophysical results of Kadanwari-10 to confirm it. Density section is generated and reservoir zone is marked on it by low value of density. Shear velocities are used to generate the shear impedance model to get the shear impedance section after seismic inversion. This S impedance is used along with P impedance to find the Lambda-Rho and Mu-Rho section. Reservoir zone is picked by low value of Lambda-Rho with corresponding high value of Mu-rho. Compressional wave velocity and shear wave velocity is used to find the Vp/Vs section, reservoir zone is picked here by low value of Vp/Vs.

Table of Contents



CHAPTER NO # 1	1
INTRODUCTION.....	1
1.1 Introduction to the study Area	1
1.2 Objectives of Study.....	2
1.3 Data used	2
1.4 Data formats.....	2
1.5 Seismic Data	2
1.5.1 General Acquisition Parameters of 2D seismic survey.....	2
1.5.2 Seismic data	3
1.5.2.1 2D Seismic data	3
1.5.2.2 3D Seismic data	3
1.6 Well Data.....	4
1.7 Base Map	4
CHAPTER # 2	6
GENERAL GEOLOGY AND STRATIGRAPHY	6
2.1 Introduction.....	6
2.2 Regional Setting and Tectonics	6
2.3 Central Indus Basin.....	7
2.3.1 Geological Boundaries of Central Indus Basin.....	8
2.4 Geology of the Study Area	8
2.5 Depositional setting and Stratigraphy.....	8
2.6 Petroleum Geology of the Area	10
2.6.1 Source Rocks.....	10
2.6.2 Reservoir Rocks	10
2.6.3 Seal (Cap) Rocks.....	10
CHAPTER # 3	11
SEISMIC INTERPRETATION	11
3.1 Introduction.....	11
3.1.1 Structural Analysis.....	11
3.1.2 Stratigraphic Analysis	11
3.2 Work Procedure	12
3.3 Synthetic Seismogram	12

3.4 Horizon and Fault interpretation.....	15
3.5 Contour maps.....	18
3.6 Time contour maps	18
3.6.1 Time contour map of Upper Goru.....	18
3.6.2 Time contour map of Lower Goru	19
3.6.3 Time contour map of G Sand	20
3.6.4 Time contour map of E Sand	21
3.7 Velocity contour maps.....	22
3.7.1 Velocity contour map of Upper Goru	22
3.7.2 Velocity contour map of Lower Goru.....	22
3.7.3 Velocity contour map of G Sand.....	25
3.7.4 Velocity contour map of E Sand	26
3.8 Depth contour maps.....	27
3.8.1 Depth contour map of Upper Goru	27
3.8.2 Depth contour map of Lower Goru.....	28
3.8.3 Depth contour map of G Sand.....	29
3.8.4 Depth contour map of E Sand	30
CHAPTER # 4	31
PETROPHYSICAL ANALYSIS	31
4.1 Petrophysical Analysis.....	31
4.2 Methodology for Petrophysical analysis	31
4.2.1 Calculation of volume of shale	31
4.2.2 Porosity Calculation.....	32
4.2.3 Formation temperature.....	33
4.2.4 Saturation of water	33
4.2.5 Hydrocarbon Saturation	33
4.2.6 Zone calculation.....	33
4.3 Petrophysical results of Kadanwari-08	34
4.4 Petrophysical results of Kadanwari-10.....	36
4.5 Facies Analysis	38
4.5.1 LMR cross plot analysis.....	38
4.5.2 Lambda-Rho Vs P-Impedance	38
4.5.3 Density Vs Poisson ratio	40

4.5.4 P-impedance Vs Vp/Vs.....	40
CHAPTER # 5	42
5.1 Fault Seal Analysis	42
5.1.1 Introduction.....	42
5.1.2 Methodology	42
5.1.3 Juxtaposition of the lithologies	43
5.1.4 Shale-Gouge Ratio	44
5.1.5 Conclusion	44
5.2 Seismic Attribute Analysis	45
5.2.1: Reflection Strength Attribute (Envelop of trace/Instantaneous Amplitude).....	45
5.2.2 Instantaneous Phase	46
5.2.3 Average energy	47
CHAPTER # 6.....	49
SEISMIC INVERSION	49
6.1 Introduction.....	49
6.2 Methodology.....	49
6.2.1 Model Based Inversion	49
6.2.2 Inversion Analysis.....	51
6.3 Density Section.....	53
6.4 Porosity calculation	54
6.5 Lambda-Mu-Rho calculation.....	57
6.6 Vp/Vs calculation	58
CONCLUSION.....	60
REFERENCES	61



List of Figures

Figure 1.1: Map of Pakistan highlighting the area of study, along with satellite imagery of study area (Berger et al., 2009).	1
Figure 1.2: Base map of study area.	5
Figure 2.1: Division of central Indus basin (Raza et al., 1989).	7
Figure 3.1: Interpretation work flow.	12
Figure 3.2: Synthetic seismogram of well Kadanwari-10.	13
Figure 3.3: Synthetic seismogram of well Kadanwari-08.	14
Figure 3.4: Overlaid synthetic seismogram of Kadanwari-08 on seismic line TJ89-508.	15
Figure 3.5: Interpreted seismic line TJ89-508.	16
Figure 3.6: Interpreted seismic line TJ89-512.	16
Figure 3.7: Interpreted seismic line TJ90-709.	17
Figure 3.8: Interpreted seismic 3D Inline 2012.	17
Figure 3.9: Time contour map of Upper Goru.	18
Figure 3.10: Time contour map of Lower Goru.	19
Figure 3.11: Time contour map of G Sand.	20
Figure 3.12: Time contour map of E Sand.	21
Figure 3.13: Velocity contour map of Upper Goru.	23
Figure 3.14: Velocity contour map of Lower Goru.	24
Figure 3.15: Velocity contour map of G Sand.	25
Figure 3.16: Velocity contour map of E Sand.	26
Figure 3.17: Depth contour map of Upper Goru.	27
Figure 3.18: Depth contour map of Lower Goru.	28
Figure 3.19: Depth contour map of G Sand.	29
Figure 3.20: Depth contour map of E Sand.	30
Figure 4.1: Petrophysical Analysis of well Kadanwari-08.	35
Figure 4.2: Petrophysical Analysis of well Kadanwari-10.	37
Figure 4.3: Lambda-Mu-Rho cross plot.	39
Figure 4.4: Cross plot between Lambda-Rho and P-Impedance.	39
Figure 4.5: Density Vs Poisson ratio cross plot.	40
Figure 4.6: Cross plot between P-impedance and V_p/V_s	41
Figure 5.1: Shale gouge ratio method.	43
Figure 5.2: Juxtaposition diagram showing the Lithological juxtaposition.	44
Figure 5.3: Reflection strength attribute applied on TJ89-512.	46
Figure 5.4: Instantaneous phase attribute applied on seismic line TJ89-512.	47
Figure 5.5: Average energy attribute applied on seismic line TJ89-512.	48
Figure 6.1: Model Based Inversion work flow.	50
Figure 6.2: Initial impedance model.	51
Figure 6.3: Inversion analysis at well Kadanwari-10.	52
Figure 6.4: Inverted section of Inline 2004.	52
Figure 6.5: Inverted Density section of seismic inline 2004.	53
Figure 6.6: Density distribution map of G Sand.	54

Figure 6.7: Cross plot between Acoustic Impedance and Porosity 55
Figure 6.8: Porosity section of Inline 2004 55
Figure 6.9: Porosity distribution map of G Sand..... 56
Figure 6.10: Lambda-Rho section of seismic Inline 2004. 57
Figure 6.11: Mu-Rho section of seismic inline 2004. 58
Figure 6.12: Vp/Vs section of seismic inline 2004. 59

List of Tables

Table 1.1: Acquisition and processing parameters of 2D seismic data.	2
Table 1.2: Orientation, Nature of 2D seismic lines along with well.	3
Table 1.3: 3D seismic data detail.	3
Table 1.4: Information of the wells used for interpretation.....	4
Table 2.1: Stratigraphy of the study area.	9
Table 4.1: Petrophysical summary of well Kadanwari-08.	34
Table 4.2: Petrophysical summary of well Kadanwari-10.	36



INTRODUCTION

1.1 Introduction to the study Area

Geographically the area of study “Kadanwari Gas Field” is located 35km south of Miano field. It was discovered by Eni Pakistan in year 1989. It is a gas field with condensate and lies in Middle Indus Basin of Pakistan. It is surrounded by different gas fields such as Miano, Sawan and Latif gas field.

Latitude : 26°51’54” N - 27°16’47” N

Longitude : 68°58’58” E - 69°21’56” E

A map of Pakistan highlighting the Kadanwari area is given in Figure (1.1).

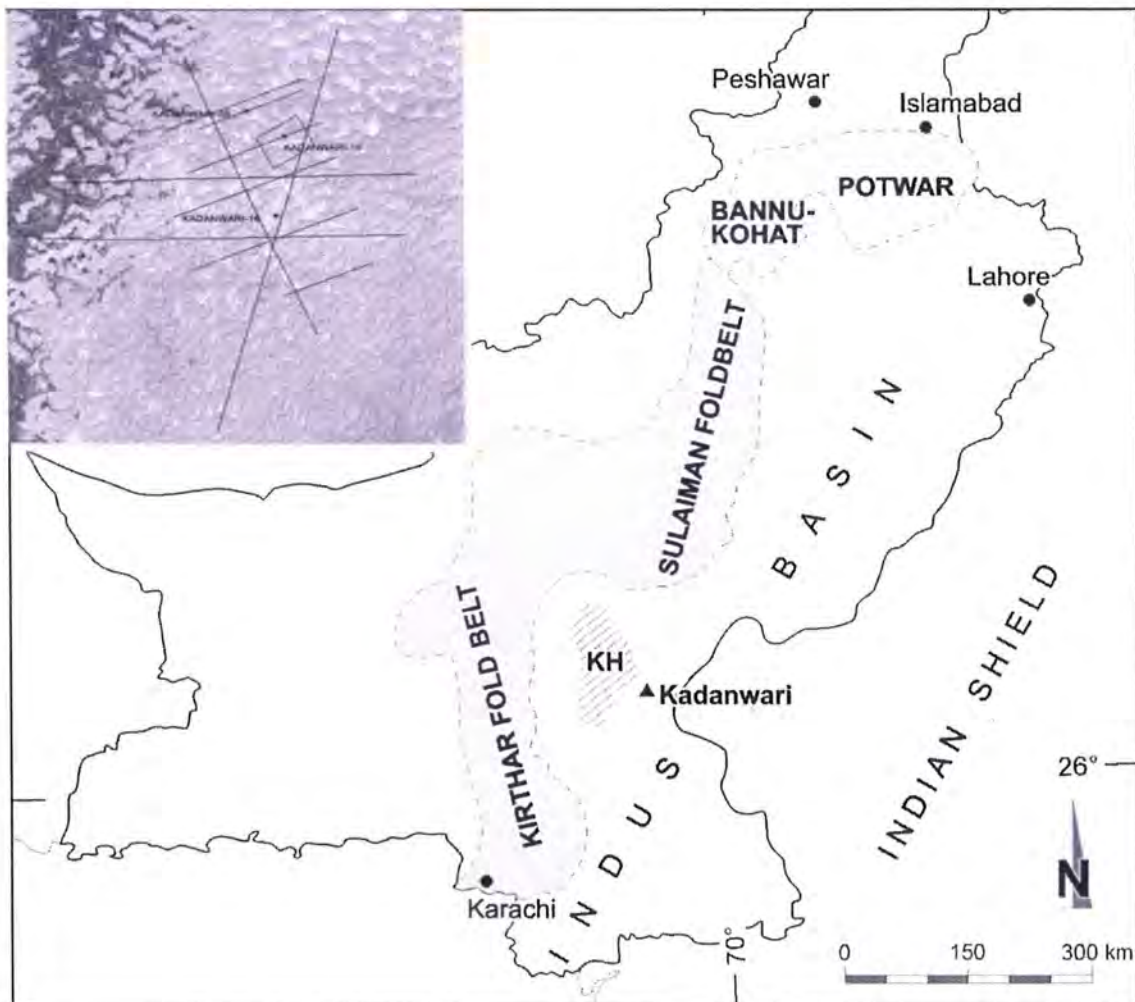


Figure 1.1: Map of Pakistan highlighting the area of study, along with satellite imagery of study area. (Berger et al., 2009)

1.5.2 Seismic data

The detail about the seismic data (2D/3D) is given below:

1.5.2.1 2D Seismic data

Detail of 2D seismic data is given in Table (1.2).

Table 1.2: Orientation, Nature of 2D seismic lines along with well.

Serial No.	Line Name	Orientation	Nature	Well
01	TJ89-508	NW-SE	Dip	Kadanwari-08
02	TJ89-512	SE-NW	Dip	Kadanwari-10
03	TJ89-516	SE-NW	Dip	
04	TJ89-522	SW-NE	Dip	
05	TJ89-528	NW-SE	Dip	
06	TJ90-709	SE-NW	Strike	
07	TJ91-806	E-W	Dip	
08	TJ88-204	NW-SE	Dip	
09	TJ88-206	NE-SW	Dip	
10	TJ88-207	SW-NE	Strike	

1.5.2.2 3D Seismic data

Detail of 3D seismic data is given in Table (1.3).

Table 1.3:3D seismic data detail.

Line	Start	End	Total	Bin Spacing
Inline	1962	2082	121	25
Xline	1896	2058	169	25

1.6 Well Data

Well data is very important in interpretation because it confirm the depth of formations on seismic section by correlating seismic data with well data and also for finding the petrophysical properties of wells. Details of well used for the interpretation are given in the Table (1.4).

Table 1.4: Information of the wells used for interpretation.

Well name	Latitude	Longitude	TD	KB	Status
Kadanwari-08	27.197081	69.199669	3423	78.7	ABD
Kadanwari-10	27.172705	69.236612	3545	61.82	Gas
Kadanwari16	27.09411	69.22973	3520	91	ABD

1.7 Base Map

A base map shows the Boundary of field area, seismic survey lines, wells and other cultural data with respect to any coordinate reference system. It is the most important thing because after interpretation we have to post the time, depth contour on this map. Figure (1.2) shows the base map of the study area.

CHAPTER # 2

GENERAL GEOLOGY AND STRATIGRAPHY

2.1 Introduction

Interpretation of seismic data is related to the geology of that area, so we must have better understanding with the geology of study area before start of interpretation because different lithologies have same seismic signature mostly, we can differentiate it if we have a good knowledge of area geology. Then we can mark the horizons and faults accurately on seismic section and also the position of unconformities.

2.2 Regional Setting and Tectonics

Pakistan is located at the junction of Indian Plate, Arabian Plate and Eurasian Plate. Pakistan lies at the Northwest boundary of the Indian Plate. The Indian Plate is under thrusting beneath the Eurasian Plate since Eocene time. This collision causing uplift that produces the highest peaks in the world including the Himalayan, the Karakorum, the Pamir and the Hindu Kush ranges. We can study transform plate boundary which is Chaman fault, fossil island arcs which are Chagai, Kohistan and Ladakh, Suture zones related to subduction such as Shyok and Indus suture, Makran deformed plate margin and trench arc system with active plate subduction in this small region. Rocks sequences exposed here includes plutonic and metamorphic rocks of Precambrian age, Paleozoic, Mesozoic and Paleogene pericretonic shelf deposits which form the mountain fold belt and cover of platform area, and thick and extensive pile of Siwaliks (Neogene molasses) which fills the foredeep. (Kazmi et al.,1997)

There are three main sedimentary basins in Pakistan.

- Indus Basin
- Baluchistan Basin
- Kakar-Khorasan Basin or Pashin Basin.

Indus Basin is the largest basin of Pakistan. The main feature which control the sedimentation of Indus Basin up to Jurassic is Indian shield in the form of Kirana Hills and Nagar Parkar Ridge. (Kadri, 1995) Sargodha high divides the Indus basin into two Sub-Basins.

- Upper Indus basin
It is further divided into Kohat sub-basin and Potwar sub-basin.
- Lower Indus basin
Khairpur-Jacobabad High further divides the lower Indus basin into Central Indus basin and Southern Indus basin.

2.3 Central Indus Basin

It is separated from Upper Indus Basin by Sargodha High. Oldest rock which is exposed in this basin is Walgai Formation which is of Triassic age and the oldest rock which is penetrated through wells is salt Range formation which is of Precambrian age. The basin is divided into three features from east to west.

- Punjab Platform
- Sulaiman Depression
- Sulaiman Fold Belt

Figure (2.1) shows the division of Central Indus Basin.

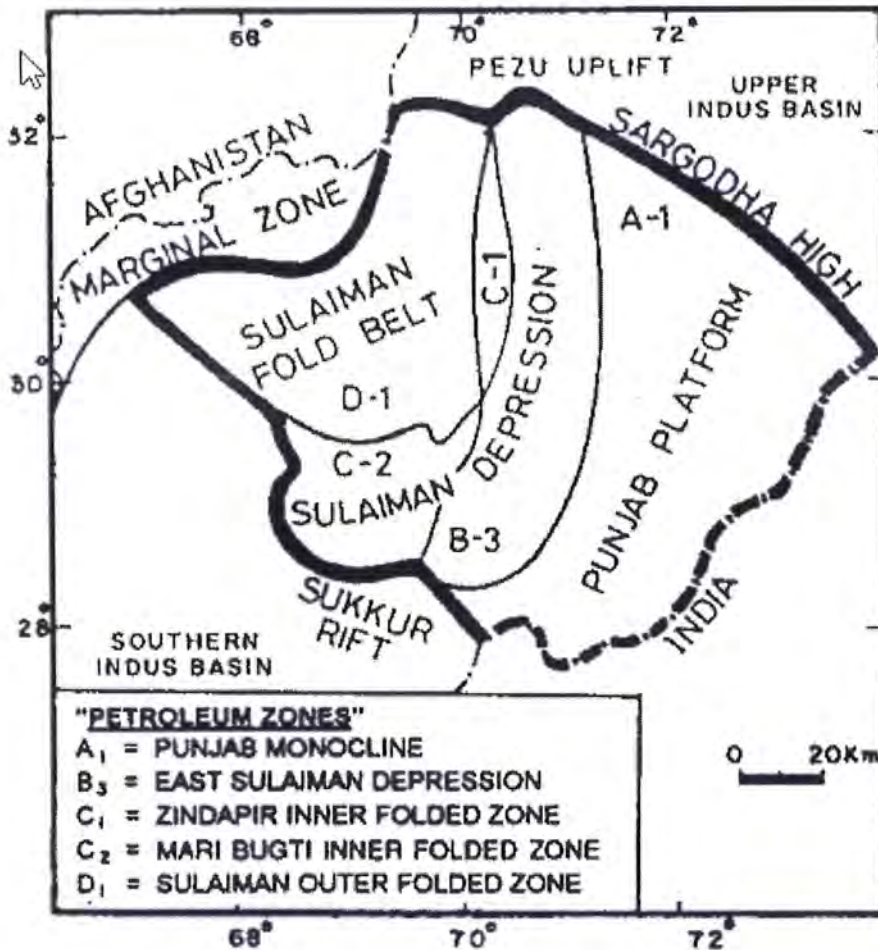


Figure 2.1: Division of central Indus basin. (Raza et al, 1989)

2.3.1 Geological Boundaries of Central Indus Basin

Geological boundaries of Central Indus Basin are given as: (Kadri, 1995)

- Marginal zone of Indian plate in the west.
- Indian Shield in the east.
- Sukkur Rift in the south.
- Sargodha High and Pezu Uplift in the north.

2.4 Geology of the Study Area

Kadanwari field lies in Central Indus Basin of Pakistan on the South-Eastern flank of Khairpur-Jacobabad High. Geological Structure forms in this field are due to three main tectonic events. (Nasir et al., 2007)

- Late Cretaceous uplift and erosion, the axis of uplift have NNE-SSW orientation.
- Right lateral Wrench faults, which have NNW-SSE orientation and shows flower structure.
- Late Tertiary to recent uplift of the Jacobabad high, which mainly develops the stratigraphic and structural traps in this area.

2.5 Depositional setting and Stratigraphy

Stratigraphy of this area includes Mesozoic, Tertiary and Quaternary lithologies. Unconformity is present between the base of Permian and Tertiary. Jurassic rocks in this area show the deposition in early rifting stage. Ranikot clastics were deposited during early Paleocene collision, which is followed by Eocene carbonates that includes Sui Main Limestone. It was deposited on shallow water carbonate platform with sporadic influx of clastics material. Medium to Coarse grained sandstones in a shallow marine setting constitute Lower Goru Formation. (Majid et al., 2016)

Table 2.1: Stratigraphy of the study area.

Age	Formation	Lithology	
Pliocene	Siwaliks	Sandstone, Claystone	
Oligocene	Nari	Shale, Sandstone	
Eocene	Drazinda	Limestone, Marl	
	Pirkoh	Limestone	
	Sirki	Claystone, Limestone	
	Habib Rahi	Limestone, Claystone	
	Ghazij	Claystone, Limestone	
	Sui Main Limestone	Limestone	
Paleocene	Dughan	Limestone, Marl, Sandstone	
	Ranikot	Claystone, Sandstone, Marl	
Cretaceous	Pab	Sandstone	
	Mughal Kot	Mudstone, Shale	
	Parh	Limestone, Marl, Shale	
	Upper Goru	Limestone, Claystone, Marl, Siltstone, Sandstone	
	Lower Goru		Claystone, Siltstone, Sandstone
		H Sand	Claystone, Siltstone, Sandstone
		G Sand	Claystone, Siltstone, Sandstone
		F Sand	Claystone, Siltstone, Sandstone
		E Sand	Claystone, Sandstone
		D Sand	Claystone, Sandstone
		C Sand	Claystone, Siltstone, Sandstone
B Sand		Claystone, Siltstone, Sandstone	
Sember	Shale, Limestone		
Jurassic	Chiltan	Limestone	



2.6 Petroleum Geology of the Area

The traps in the study are structural and related to extensional and transtentional features. Structure is dominated by wrench faults which are associated with dextral shear of few 10 of meters. Horst structures in this area is due to late cretaceous to tertiary age movement along left lateral transpressive wrench system. Kadanwari arch is structurally the highest part and lies between two strike-slip faults, it's the core area of Kadanwari field. To the east of this arch some wells are successfully drilled on E sand level.

2.6.1 Source Rocks

Organic rich shales in Sember formation of lower Cretaceous age are the source of hydrocarbon generation in this area. It contains type III kerogen which is capable of generating gas. The gas prone, pro-delta marine shales of Lower Goru formation are also most likely source of gas in this area.

2.6.2 Reservoir Rocks

Lower Goru Sands acts as reservoir in this area. Lower Goru sand is further divided into sub units. Each company have different classification, ENI divides it into seven sub units named from B-H. In this area E and G sands are main producing sands but D and F sands are also producing in this area. G and E sand is good quality reservoir having porosity value up to 18-22% and permeability value from 200 to 2000mD.

2.6.3 Seal (Cap) Rocks

Shales of Upper Goru formation and within Lower Goru formation act as a seal for underlying Lower Goru sands which are acting as reservoir.

CHAPTER # 3

SEISMIC INTERPRETATION

3.1 Introduction

Seismic interpretation is a way to get information about the structures in the subsurface from processed seismic data. Its main objective is to prepare contour maps which show the trend of reflectors that are marked on seismic sections. They help us in finding the possible zones of hydrocarbon accumulation in the subsurface sedimentary rocks. So, it's the transformation of seismic data into structural picture by contouring the subsurface horizons. For better interpretation, we must have a good knowledge about the geological history of the area.

In seismic interpretation, we pick the horizon and mark it in lateral direction and pick the discontinuity which is may be structural or stratigraphic.

There are two main approaches for interpretation of seismic sections:

- Structural Analysis.
- Stratigraphic Analysis

3.1.1 Structural Analysis

It is used for identification of structural traps such as normal and reverse faults, anticlines.etc which are containing hydrocarbons. Mostly we perform this on the basis of two-way reflection time data and then time structural maps are constructed to represent the geometry of subsurface reflectors. Discontinuity in the reflection events indicates faults and undulation indicate folds.

3.1.2 Stratigraphic Analysis

It is used for identification of stratigraphic boundaries. Geoscientist realize that the seismic signal is too small than noise which change the shape of reflected wavelet that indicates the change in the noise which is superimposed. If noise will be attenuated the variation in the wavelet shape indicates the variation in the reflectivity of the earth which represents stratigraphic changes. It's very difficult to differentiate whether the waveform shape changes due to noise or due to stratigraphic variation. It is very important to enhance the understanding with the geology of that area and to find out the prospect zone for accumulation of hydrocarbons.

It is performed on different scale. On regional scale, stratigraphic interpretation is used to find the system and environment of deposition which is called seismic sequence analysis. On local scale, it is used to examine each trace individually to find out where the change in the stratigraphy and it is called reflection character analysis. (Mcquillin et al., 1984)

3.2 Work Procedure

Seismic data which is in SEG-Y format is loaded in Kingdom along with navigation and well data. Now by using well data and time depth relationship of the well, synthetic seismogram is generated which is used to identify the Horizons position on seismic sections. By locating the horizons position they are marked laterally and faults are interpreted on the basis of discontinuity in horizons. After marking the seismic line on which well is located, it is tied with strike line and then all the remaining lines are marked on the basis of strike line. After marking reflectors and faults time contour maps of the reflectors are generated. Then seismic velocities are used to generate the depth map from time contour maps. Figure (3.1) shows the whole workflow used for interpretation.

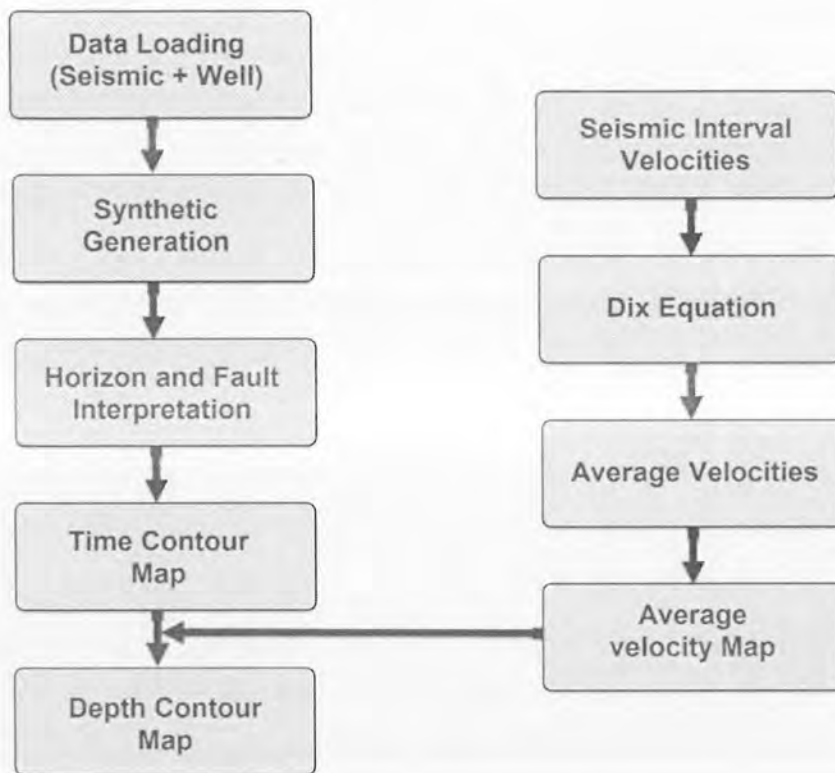


Figure 3.1: Interpretation work flow.

3.3 Synthetic Seismogram

Synthetic seismogram is seismic trace created from well data and then it is correlated with the original seismic trace near well location. It is basically 1D forward modeling. Well data which is used to generate synthetic seismogram is given as:

- Sonic log
- Density log
- Time-Depth chart
- Wavelet

Sonic log which is the measure of formation interval transit time, gives the velocity. This velocity data is used along with density log to find out the acoustic impedance values by multiplying the density and velocity value. Then impedance log is used to generate reflection coefficient series which is further convolved with the wavelet to generate synthetic trace. TD chart is used for sonic calibration. Figures (3.2) and (3.3) are showing the synthetic seismogram of Kadanwari-10 and Kadanwari-08 respectively. By using Kadanwari-08 synthetic, four horizons are picked on seismic line TJ89-508 while TJ89-512 is marked on the basis of Kadanwari-10 synthetic seismogram.

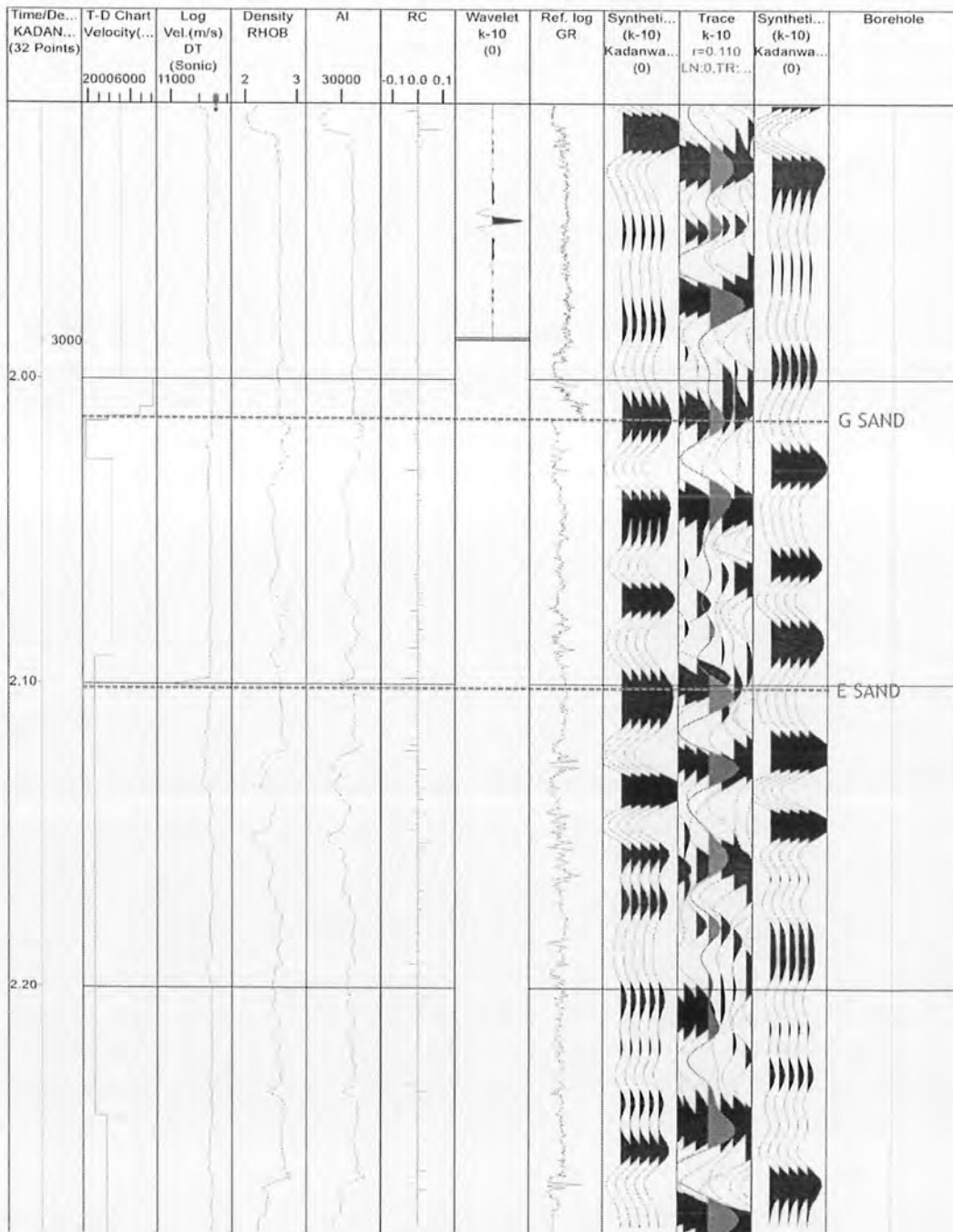


Figure 3.2: Synthetic seismogram of well Kadanwari-10.

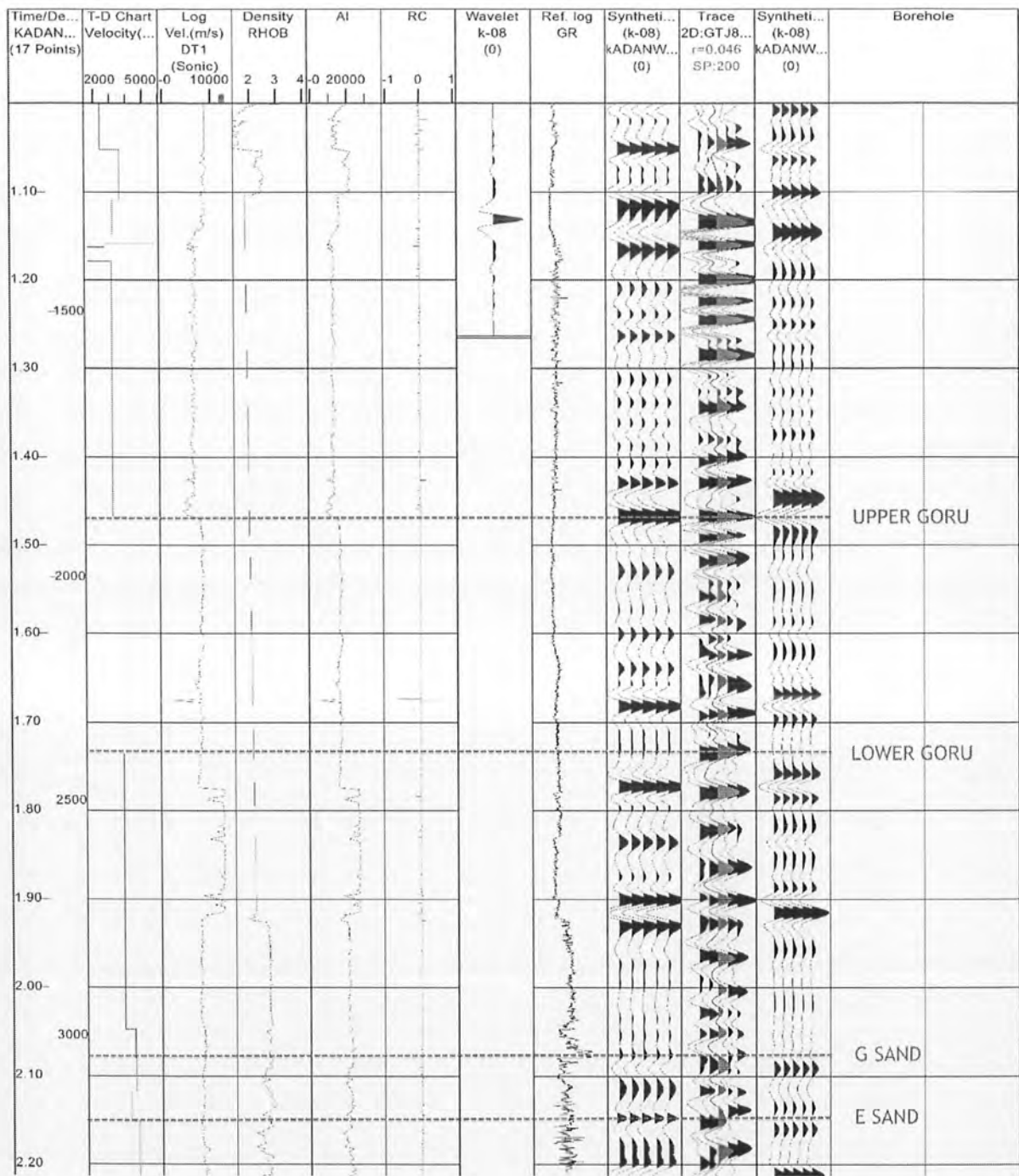


Figure 3.3: Synthetic seismogram of well Kadanwari-08.

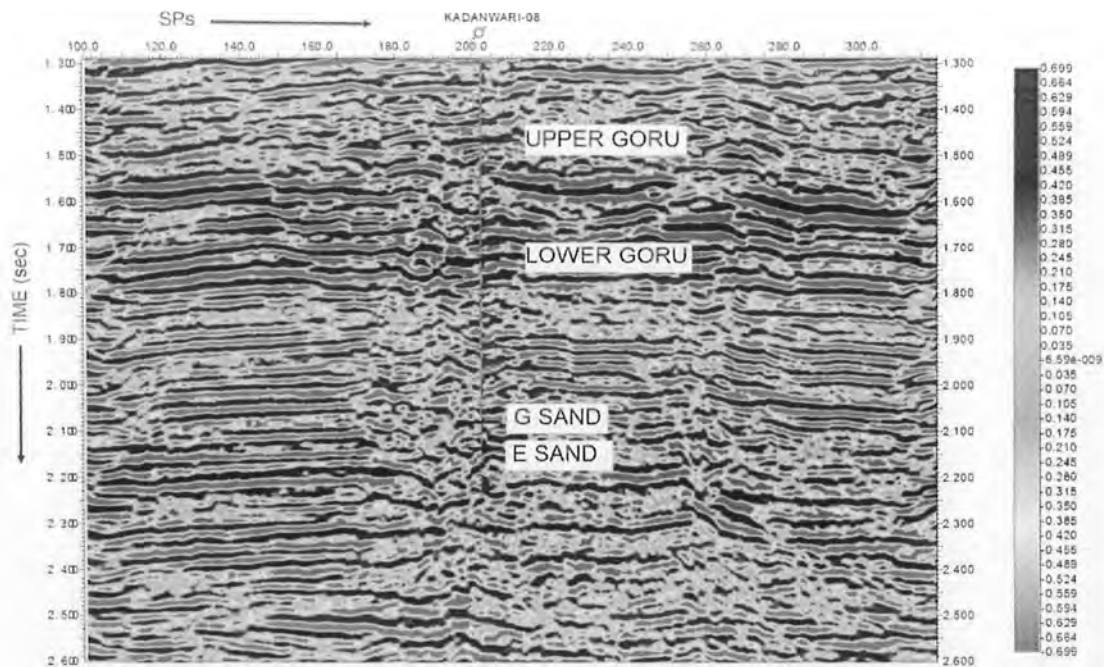


Figure 3.4: Overlaid synthetic seismogram of Kadanwari-08 on seismic line TJ89-508.

Figure (3.4) Shows the seismic section of 2D line TJ89-508 on which the synthetic seismogram of well Kadanwari-08 is displayed. Four horizons are picked on seismic section by using this synthetic.

3.4 Horizon and Fault interpretation

Based on synthetic seismograms of wells four horizons are picked on seismic sections which are given as:

- Upper Goru
- Lower Goru
- G Sand
- E Sand

During picking of horizons, faults are marked on the base of discontinuity occurs when reflectors extends laterally. Interpretation is started by marking horizon on seismic line TJ89-508, then TJ89-512 is marked and both are tied to strike line TJ90-709 to interpret this line and confirm the horizons by tied together these three seismic lines. Remaining seismic lines are interpreted by using strike line.

Figures (3.5) to (3.8) are showing the marked section of seismic lines TJ89-508, TJ89-512, TJ90-709 and Inline 2012 respectively.

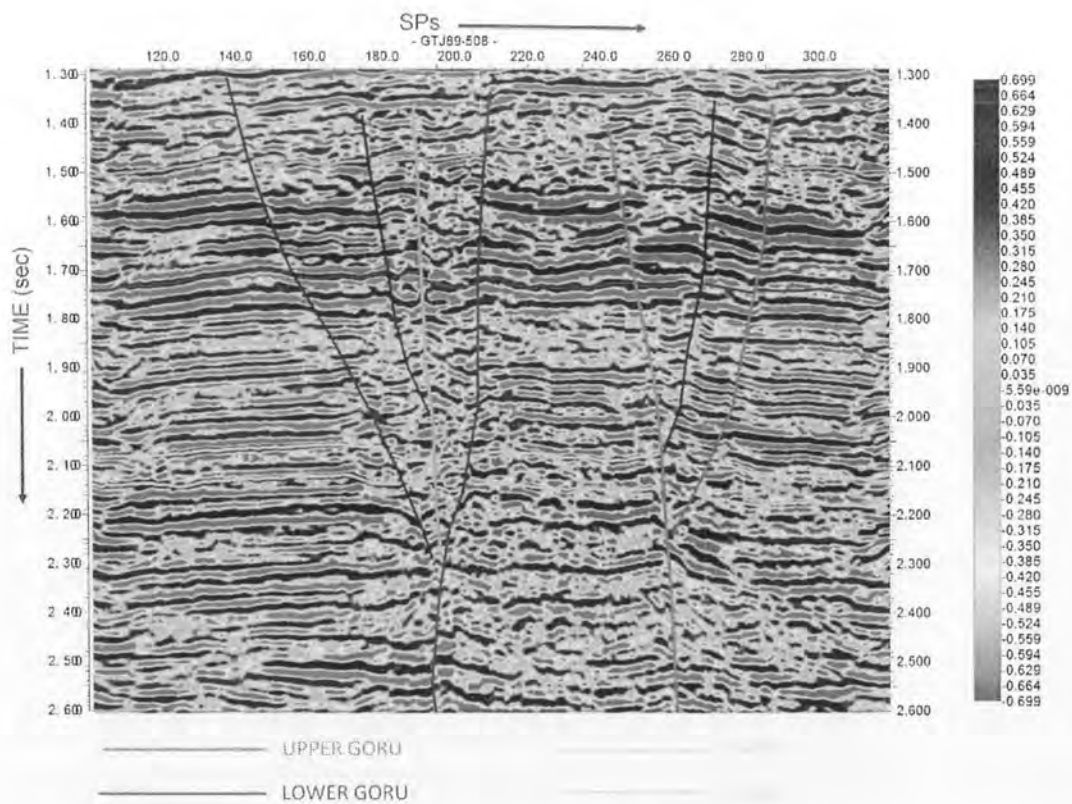


Figure 3.5: Interpreted seismic line TJ89-508.

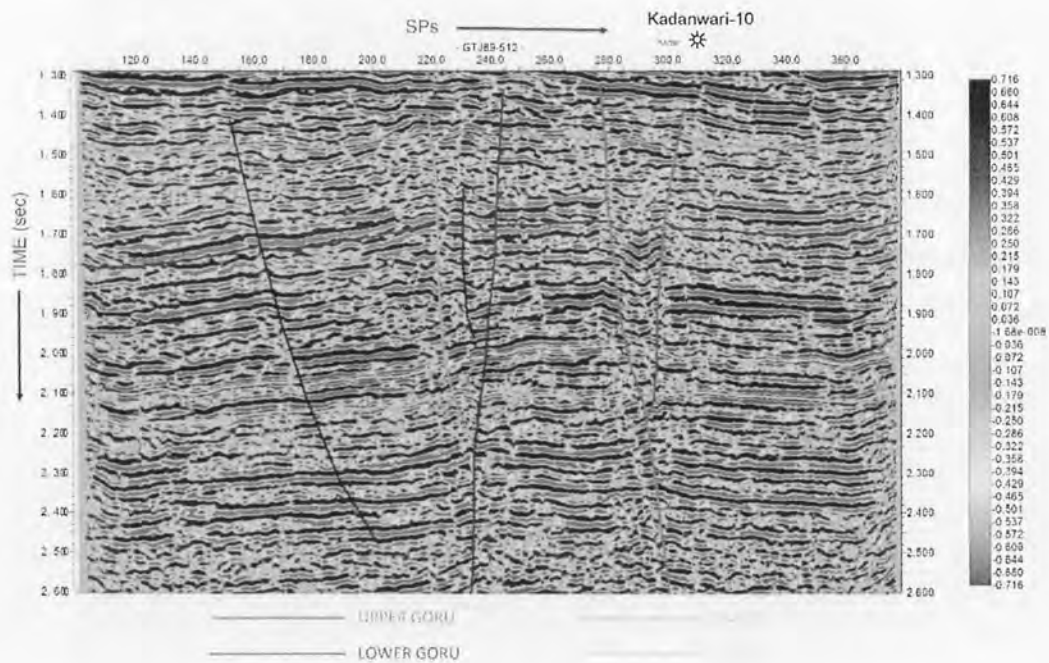


Figure 3.6: Interpreted seismic line TJ89-512.

3.5 Contour maps

Contouring is a way to represent the earth which is 3-D in the form of 2-D surfaces. They are lines of equal value. Two contour lines spacing represents the steepness if they are closer then slope is steeper. After interpretation of horizon and faults, they are represented in the form of time and depth contour maps. A map gives us information about the overall structure of the area, its closure, relief, pattern of faulting and folding, dip of the horizons.

3.6 Time contour maps

Time contour maps of all the horizons are generated using IHS Kingdom software. Seven fault polygons are marked on each map based on the trend and presence of faults on each seismic line. Maps show that in this area there are normal faults in the form of Horst and Graben. Horizons are becoming deeper in the eastern and western sides while in center they are shallow.

3.6.1 Time contour map of Upper Goru

Figure (3.9) shows the time contour map of Upper Goru. Time values are varying from 1.376 to 1.576sec. Contour interval used in this map is 0.02sec.

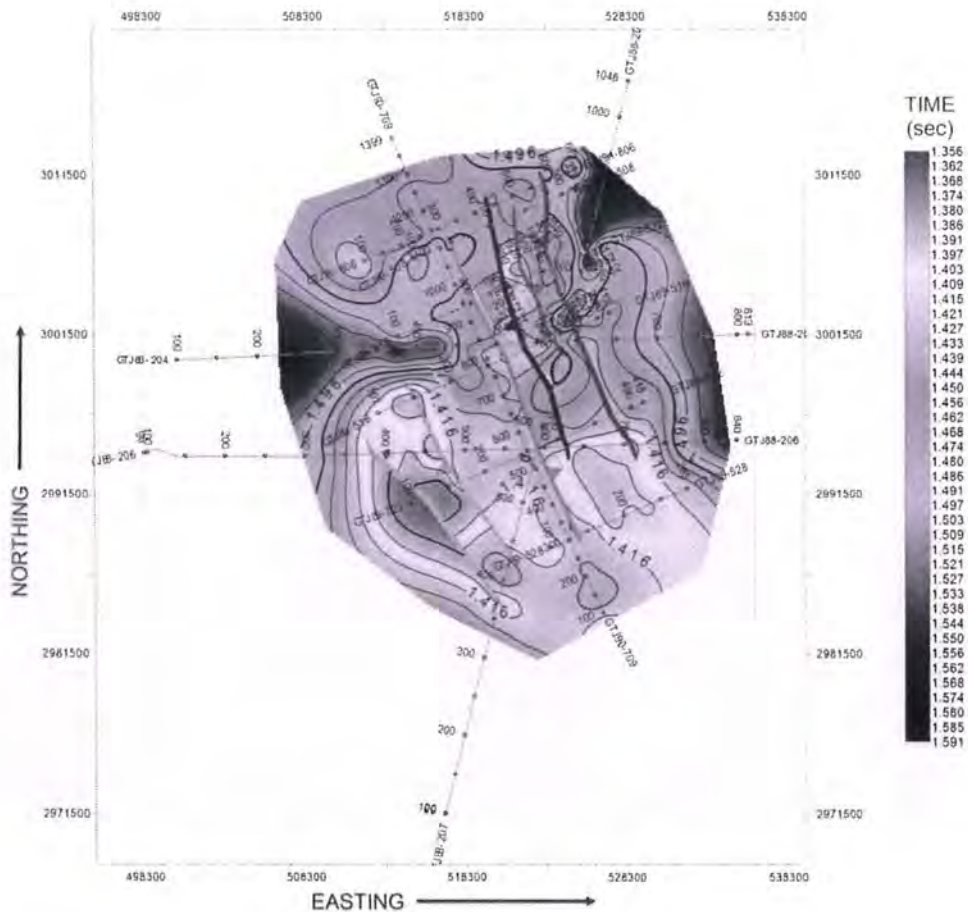


Figure 3.9: Time contour map of Upper Goru.

Seven fault polygons are display on this contour map. At the center horizon is shallow. In western and north-eastern side, it's becoming deeper while in south and south west direction its becoming shallower.

3.6.2 Time contour map of Lower Goru

Figure (3.10) shows the time contour map of Lower Goru, which is generated using interval of 0.02 sec. Time values mostly lies between 1.6 to 1.78sec. It's becoming deeper in NW direction

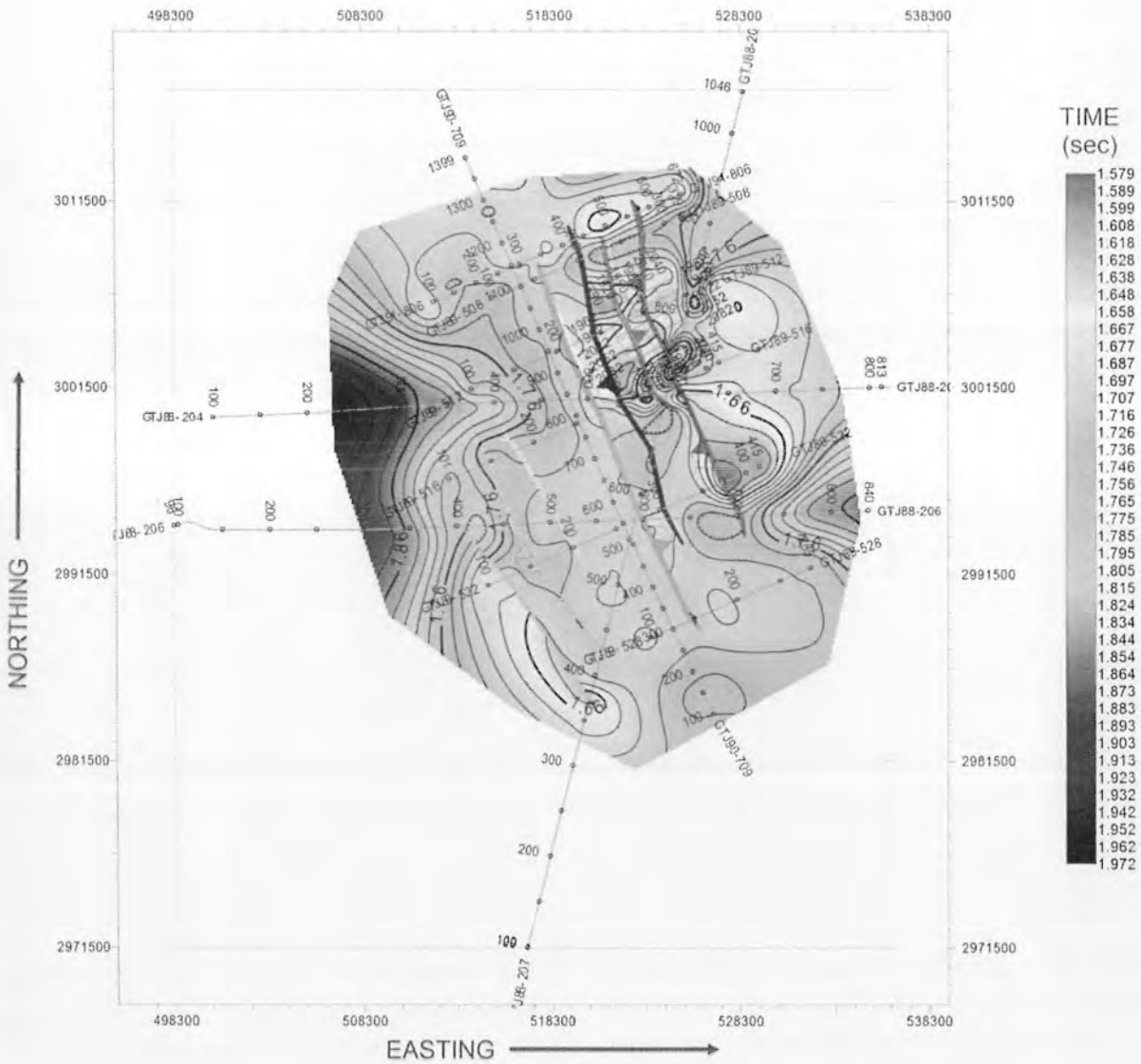


Figure 3.10: Time contour map of Lower Goru.

3.6.4 Time contour map of E Sand

Figure (3.12) shows the time contour map of E Sand. Time value is mostly changing between 2.084 to 2.215sec. Contour interval used in this map is 0.01sec

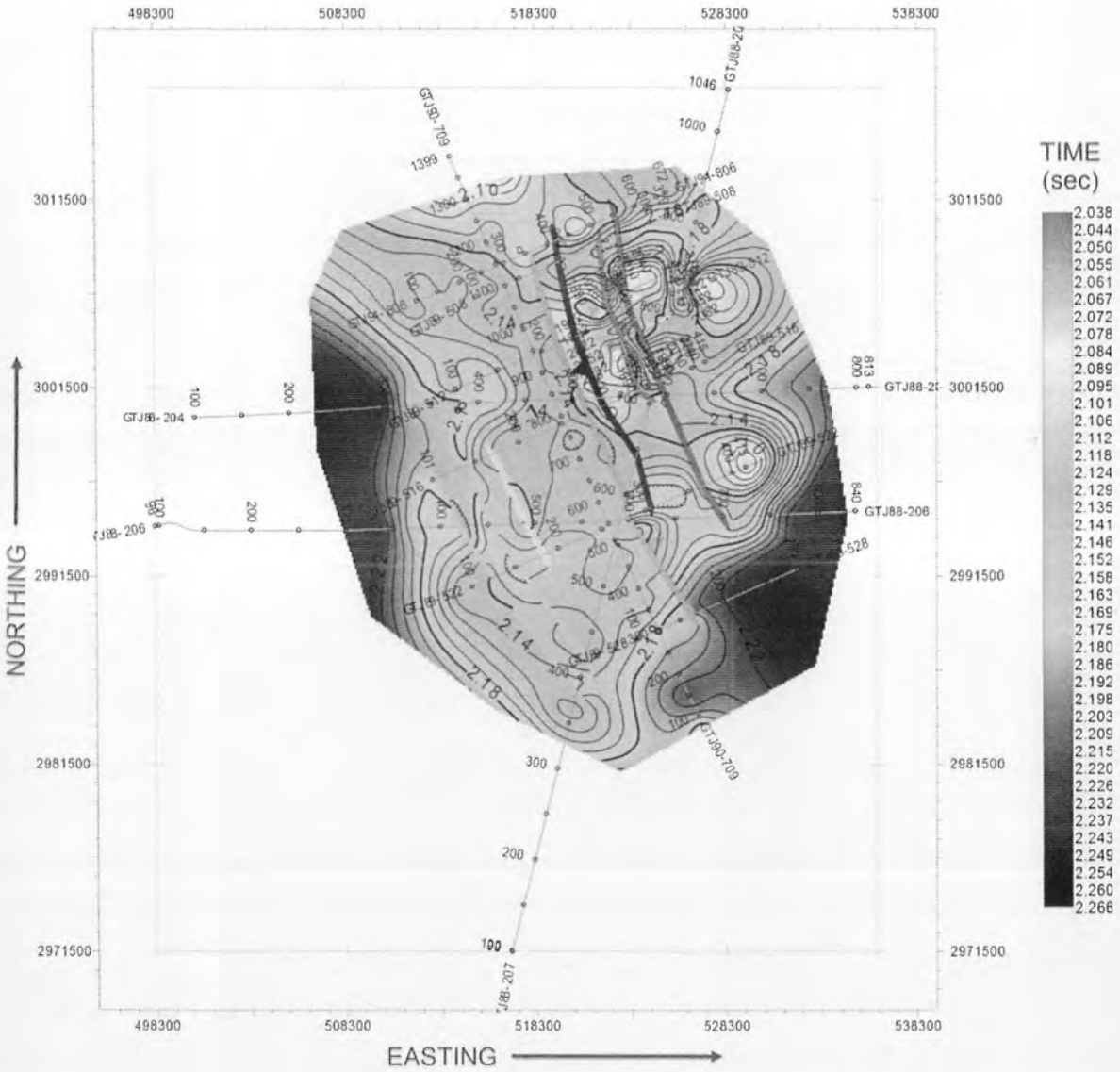


Figure 3.12: Time contour map of E Sand.

3.7 Velocity contour maps

Velocities data given on seismic sections are used to generate velocity map of the horizons. These velocities are required for converting the data from time domain to depth domain. Interval velocities from seismic section are picked and then converted into average velocities by using Dix equation (Dix, C. H., 1955) given as:

$$V_{avg,i} = \frac{\sum V_{int,i} (T_i - T_{i-1})}{T_i}$$

Where,

Vavg= Average velocity (m/s)

Vint= Interval velocity (m/s)

T= Zero off set travel time (s)

3.7.1 Velocity contour map of Upper Goru

Figure (3.13) shows the velocity map of Upper Goru, velocity values for Upper Goru is lies between 2488 to 2910m/sec. Contour interval are 60m/sec.

3.7.2 Velocity contour map of Lower Goru

Figure (3.14) shows the velocity contour map of Lower Goru, which is generated using contour interval of 50m/sec. Value of velocities are changing from 2600 to 3150m/sec. At western side value of velocity is becoming high while in SE direction its decreasing.

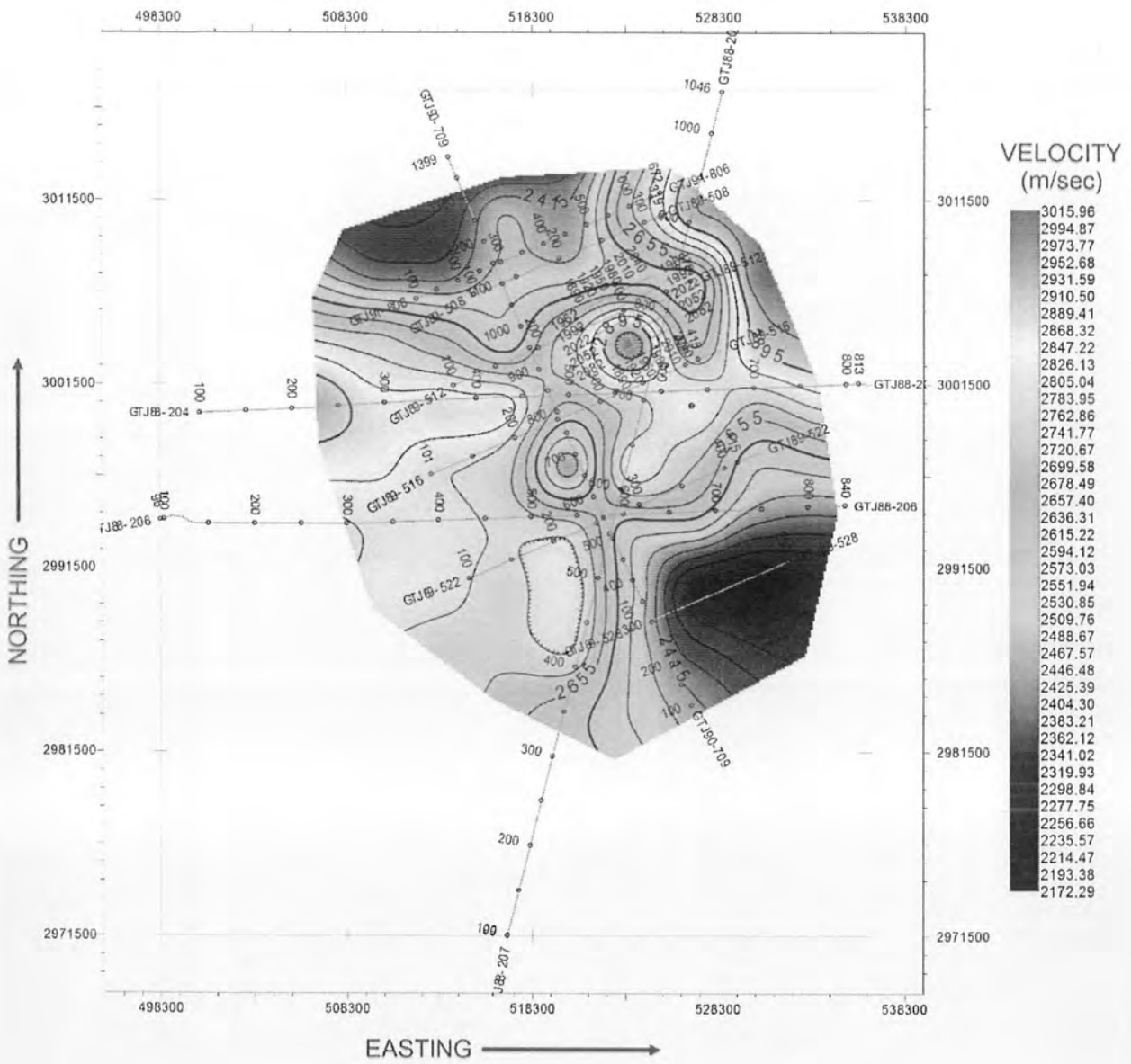


Figure 3.13: Velocity contour map of Upper Goru.

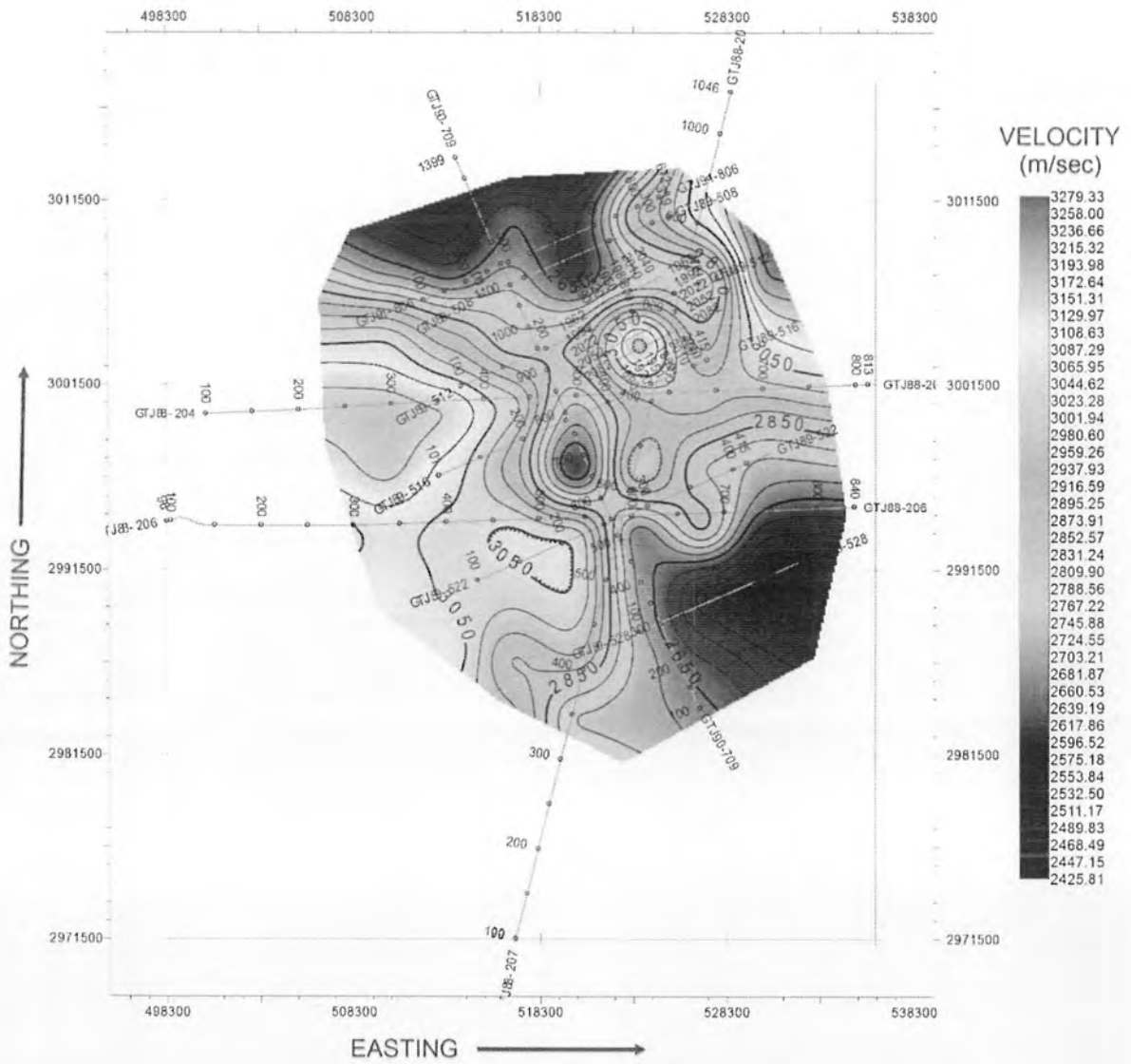


Figure 3.14: Velocity contour map of Lower Goru.

3.7.3 Velocity contour map of G Sand

Figure (3.15) shows the velocity contour map of G Sand, which is generated using contour interval of 60m/sec. Value of velocities ranging from 2900 to 3300m/sec. In central portion velocity values are low while increasing in western side.

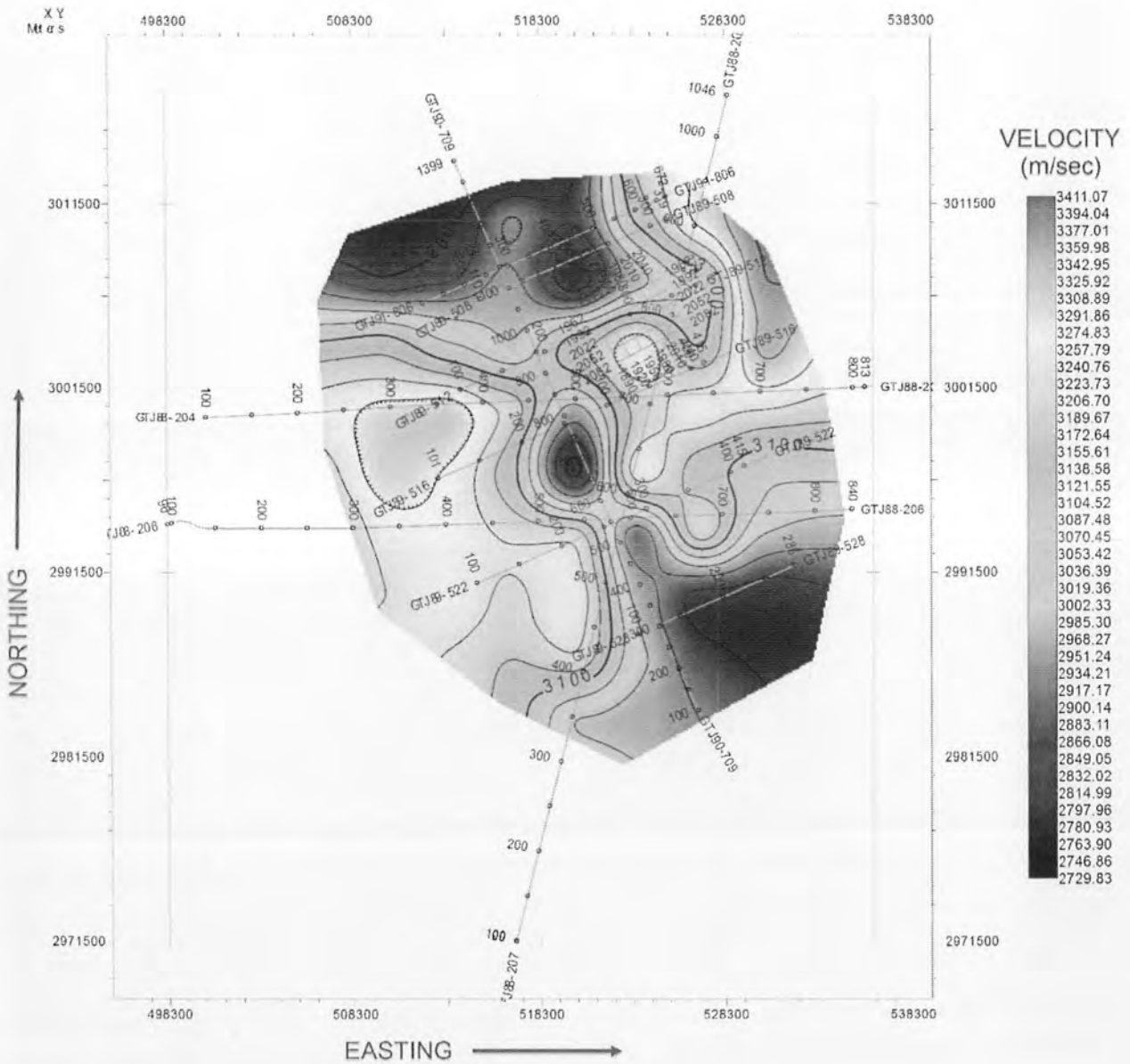


Figure 3.15: Velocity contour map of G Sand.

3.7.4 Velocity contour map of E Sand

Figure (3.16) shows the velocity map of E Sand, velocity values are varying from 2900 to 3300m/sec. Contour interval is 60m/sec. Velocity value are following the same trend as G sand contour velocity map.

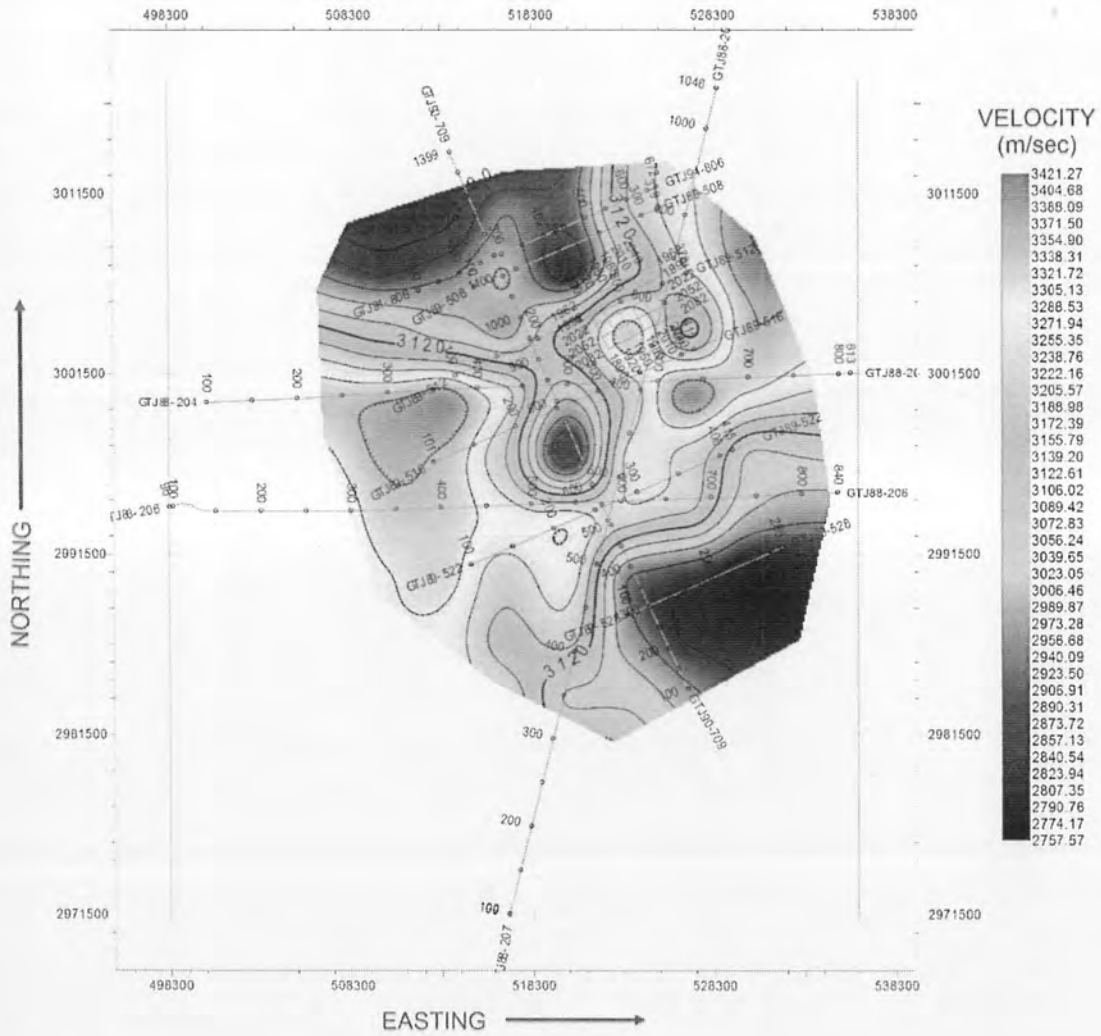


Figure 3.16: Velocity contour map of E Sand.

3.8 Depth contour maps

We must change the seismic section from time domain to depth domain because in reality subsurface structures are in depth domain. So, by using the average velocity maps time maps are converted into depth contour maps.

3.8.1 Depth contour map of Upper Goru

Figure (3.17) shows the depth map of Upper Goru, which is generated using contour interval of 60m. Depth of Upper Goru, is varying between 1700 to 2200m. Horizon is shallow in South eastern and north direction and becoming deeper in western and North-Eastern direction. In central portion it lies at moderate depth. It's confirming the Horst and Graben structure which is defining by fault polygons.

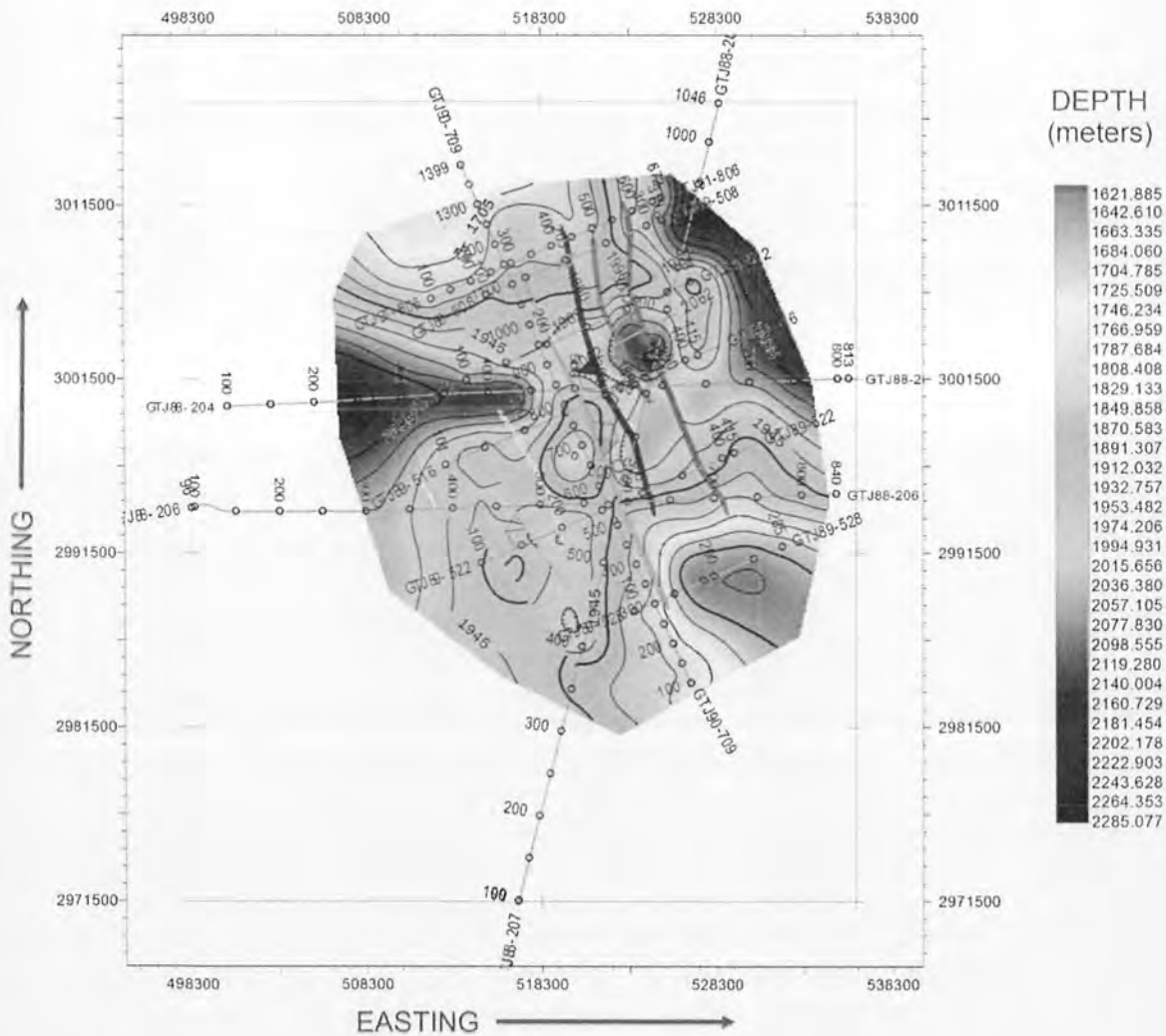


Figure 3.17: Depth contour map of Upper Goru.

3.8.2 Depth contour map of Lower Goru

Figure (3.18) shows the depth contour map of Lower Goru, depth is varying from 2300 to 2630m. Contour interval is 35m. Lower Goru is at moderate to shallow depth at center and becoming deeper in Eastern and western side but it is deeper at western side. While in South eastern side it is becoming shallower.

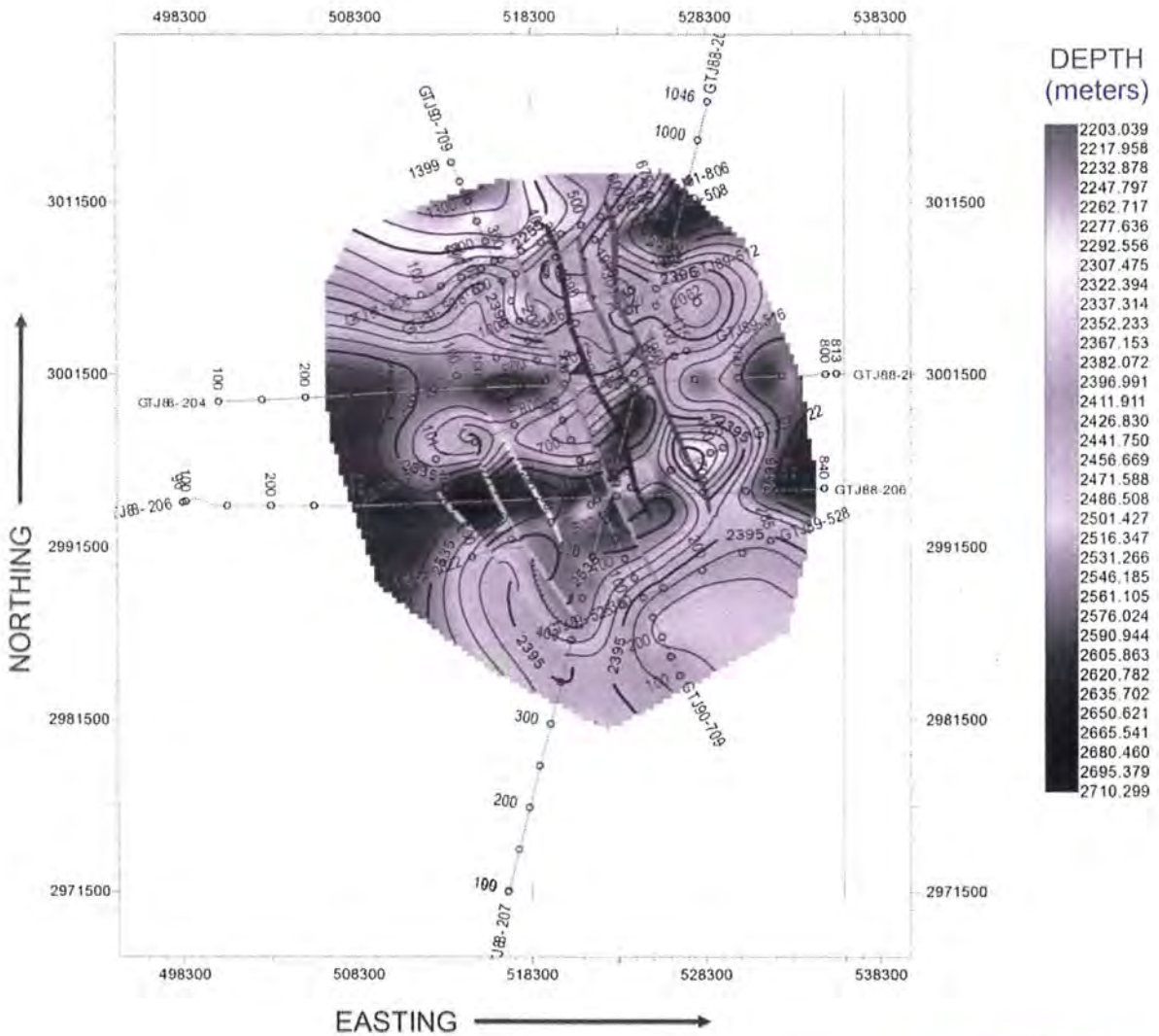


Figure 3.18: Depth contour map of Lower Goru.



3.8.3 Depth contour map of G Sand

Figure (3.19) shows the depth map of G Sand, which is generated using contour interval of 45m. Depth of G Sand is varying from 3000 to 3270m. Horizon is shallow at SW direction while its becoming deeper in western side.

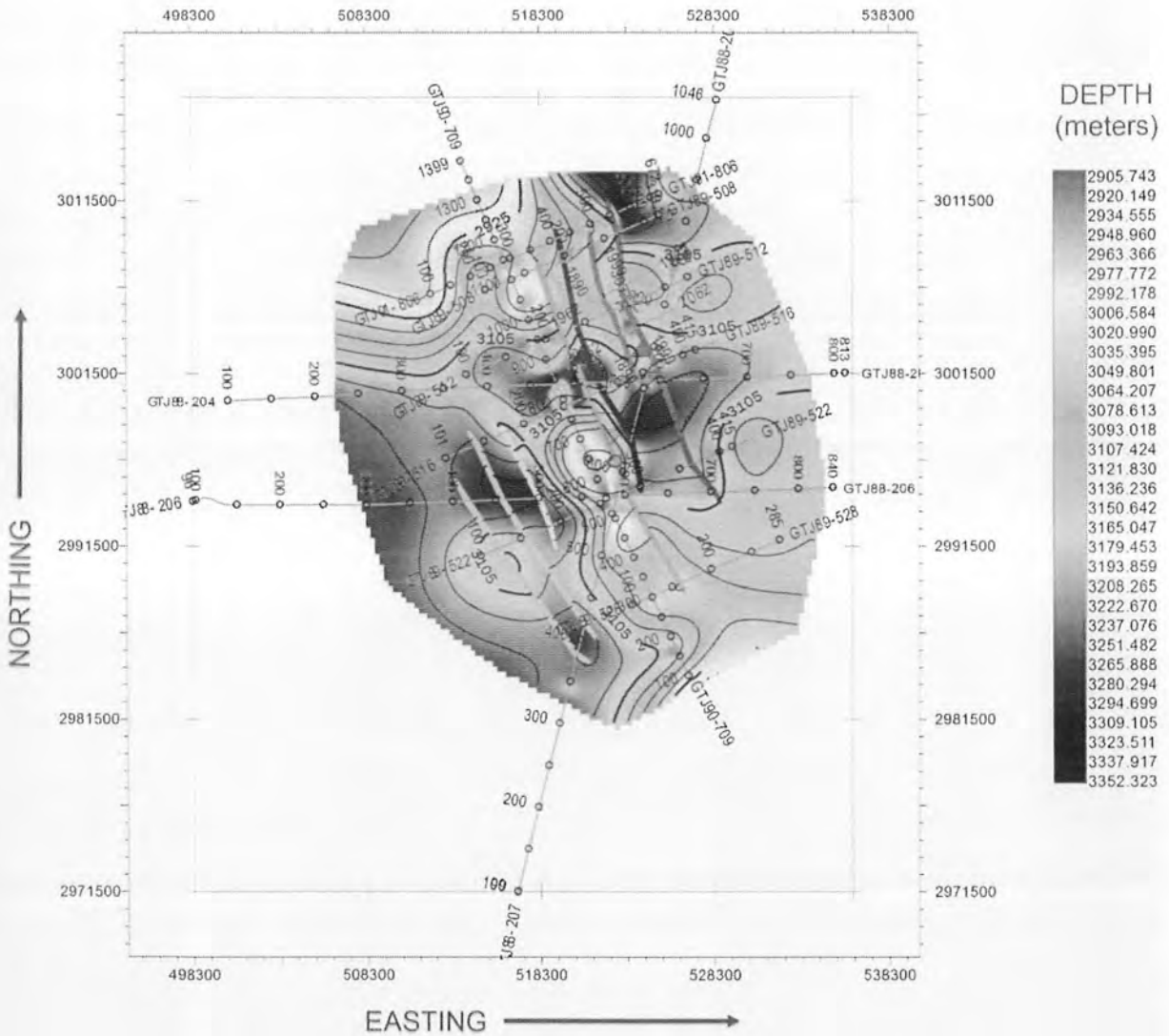


Figure 3.19: Depth contour map of G Sand

CHAPTER # 4

PETROPHYSICAL ANALYSIS

4.1 Petrophysical Analysis

Geophysical logs provide a very helpful data to geoscientist and reservoir engineers for defining the physical properties of rocks such as lithology, porosity, permeability, saturation of water and hydrocarbons, volume of shale, pore geometry, etc. (Wajid et al., 2015) In Petrophysics we use these electrical logs and it is defined as subject in which we study the physical properties of rocks. These properties are very helpful for production and development of well and reserve estimation of any field. So, we can find permeable zones for hydrocarbons and interfaces of oil, gas and water.

4.2 Methodology for Petrophysical analysis

The log data of the wells was available in Logging ASCII Standard (LAS) format. The log curves along with the data given in the well header are used to perform petrophysical analysis.

4.2.1 Calculation of volume of shale

Gamma ray log is very helpful tool to differentiate between different lithologies. By using this we can calculate volume of shale. Shale mostly represents high value of GR while sandstone, dolomite and limestone have low value of GR. Source rocks contains commonly have high radioactive content and therefore they are indicated by high GR value.

To calculate the volume of shale we have to calculate gamma ray index (I_{GR}).

$$I_{GR} = \frac{GR_{log} - GR_{min}}{GR_{max} - GR_{min}}$$

Where,

I_{GR} = Gamma Ray Index

GR_{log} = Gamma Ray reading of the formation

GR_{max} = Maximum gamma Ray (shale)

GR_{min} = Minimum gamma Ray (clean sand and carbonate)

For tertiary rocks following formula is used to find out the volume of shale V_{sh} .

$$V_{SH} = 0.083(2^{(3.71I_{GR}-1)})$$

4.2.2 Porosity Calculation

Porosity is the number of pore spaces in a rock which can hold fluids. Density, sonic and Neutron logs are used to calculate the porosity value. Before calculating porosity, shale effect is corrected for porosity logs.

Porosity can be calculated from density log

$$\Phi_D = \frac{\rho_{ma} - \rho_b}{\rho_{ma} - \rho_{mf}}$$

$$\Phi_{D_{sh}} = \frac{\rho_{ma} - \rho_{sh}}{\rho_{ma} - \rho_{mf}}$$

$$\Phi_{De} = \Phi_D - (\Phi_{D_{sh}} * V_{sh})$$

Calculation of porosity by neutron log is given as

$$\Phi_{Ne} = \Phi_N - (\Phi_{N_{sh}} * V_{sh})$$

Effective porosity by Neutron-Density log is given as

$$\Phi_{NDe} = \sqrt{\frac{\Phi_{De}^2 + \Phi_{Ne}^2}{2}}$$

Where,

ρ_{ma} = Density of matrix

ρ_b = Density log reading in zone of interest

ρ_{mf} = Density of mud filtrate

Φ = Porosity

ρ_{sh} = Shale bulk density

T = Temperature

V_{sh} = Volume of shale

Φ_D = Density porosity

Φ_{De} = Effective density porosity

Φ_{Ne} = Effective neutron porosity

Φ_{NDe} = Effective Neutron-Density porosity

4.2.3 Formation temperature

It is used in formation water resistivity calculation. The method used to calculate the formation temperature is TLI/BLI method whose formula is given as:

$$FTEMP = TLT + \frac{(BLT - TLT) * (depth - TLI)}{(BLI - TLI)}$$

TLI=Top log interval in meter

TLT=Top log temperature in °C

BLI=Bottom log interval in meter

BLT= Bottom log temperature in °C

4.2.4 Saturation of water

Archie's equation is used to calculate the saturation of water.

$$S_w = \left(\frac{a * R_w}{R_t * \Phi_t^m} \right)^{\frac{1}{n}}$$

Where

S_w = Saturation of water

a = Tortuosity factor

m = Cementation factor

n =Saturation exponent

R_w = Formation water resistivity

R_t =Formation resistivity

Φ_t = Porosity

4.2.5 Hydrocarbon Saturation

It is calculated from water saturation.

$$S_h = 1 - S_w$$

4.2.6 Zone calculation

Cut-off is applied to calculate the reservoir and pay zone. Reservoir zone is characterized based on porosity value more than 10 % and volume of shale less than 30 %. While the pay zone is defined by porosity value greater than 10%, less than 30% shale volume and saturation of water less than 75%.

4.3 Petrophysical results of Kadanwari-08

Petrophysics of well Kadanwari-08 is performed from depth 3133m to 3319m. In this depth range three horizons are present which are G Sand, F Sand and E Sand. G Sand and E Sand is the main zone of interest because these sands are target zones in this well.

Figure (4.1) shows the petrophysical results of Kadanwari-08. In this figure CALS, SP, BS and GR logs are shown in track I, Resistivity logs in track II, DT, RHOB and NPHI logs are shown in track III, volume of shale is presented in track IV, in track V porosity value is displayed, saturation of water is present in track VI, while track VII represent total rock portion, track VIII showing reservoir portion after applying volume of shale and porosity cut-off and track IX displaying pay zone after applying water saturation cut off on reservoir zone. Cross over is made between NPHI and RHOB because presence of cross-over indicate gas possibility.

In G Sand, a pay zone is present at depth 3178.422 to 3179m, here cross over between NPHI and RHOB is present, volume of shale is about 1.4%, having good porosity, and its thickness is very less about 0.58m. Water saturation in this zone is 65%. Another zone is present with thickness 0.34m. While in the remaining some zone have good porosity value and less volume of shale but they are not pay zone because saturation of water is above the cut-off value and they are about 15m thick.

In F Sand, no pay zone is present, one zone at depth 3265-3268m have cross-over with 3 m thickness and contain good porosity up to 15% with volume of shale less than 30% but the saturation of water is above the cut-off value so it's not a pay zone.

In this well thickness of E Sand is 14m. At depth 3309-3311.069m, pay zone is present where a good cross over between NPHI and RHOB is present and porosity and shale value is also below the cutoff value with water saturation value up to 50%.

As whole water saturation in reservoir zones is on average more than 90 percent and if a pay zone is present then its thickness is too small and not economical. Table 4.1 shows the whole summary of petrophysical analysis of well Kadanwari-08.

Table 4.1 Petrophysical summary of well Kadanwari-08.

Parameters	G Sand	F Sand	E Sand
Depth (m)	3133-3217	3217-3305	3305-3319
Gross (m)	84	88.2	14.3
Net (m)	70.250	43.625	7.5
Net/Gross	0.836	0.495	0.524
Net Pay	1.125	-	3.5
V _{sh} (%)	1.4	-	11.3
Porosity (%)	36.2	-	27
S _w (%)	66	-	44
S _h (%)	34	-	56

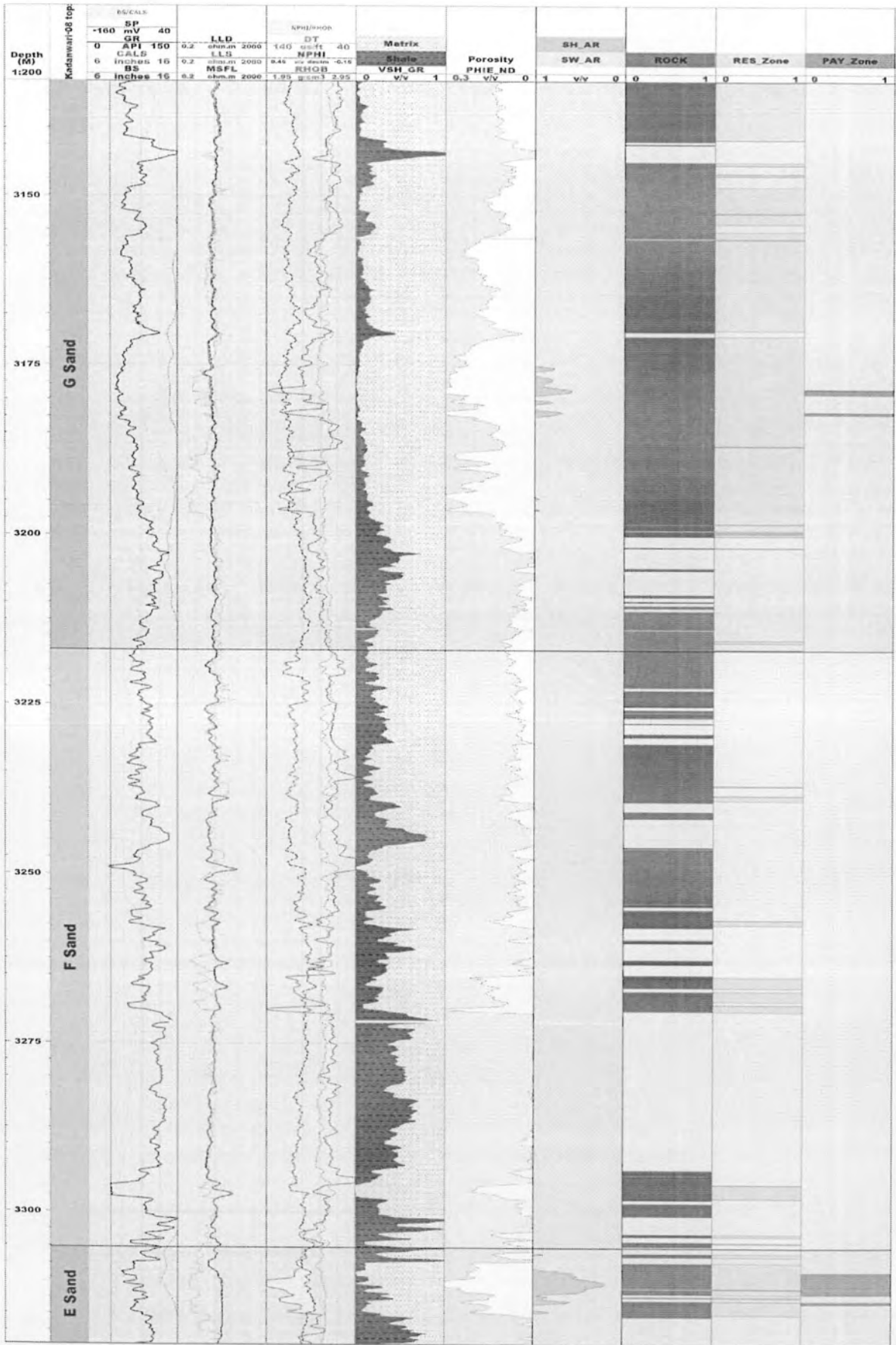


Figure 4.1: Petrophysical Analysis of well Kadanwari-08.

4.4 Petrophysical results of Kadanwari-10

Figure (4.2) shows the petrophysical analysis of well Kadanwari-10. Main target zone in this are G Sand and E Sand, which are producing reservoirs. Petrophysics is performed from 3140 to 3351m depth in which three sands of Lower Goru Formation are present (G Sand, F Sand and E Sand).

In G Sand, at depth 3140-3169m, different pay zones are present with good to very good porosity, less value of volume of shale and water saturation value upto 30%. Resistivity value is also greater with high porosity value and low value of NPHI that indicate the hydrocarbon content.

In F Sand, different pay zone is present at 3251-3257m where the value of resistivity is high, volume of shale is up to 20% with porosity level good and less water saturation value. Another portion of pay zones is from 3271-3278m.

In E Sand, good crossovers are present between 3330-3346m which indicates the presence of hydrocarbon. In this portion different pay zones are present having porosity up to excellent level with less shale and water saturation.

According to petrophysical analysis most producing Sands of Lower Goru Formation are G Sand and E Sand having net to gross 33.2% and 55.5% respectively. They have very good porosity and hydrocarbon saturation upto 80%. Table 4.2 shows the whole petrophysical summary of well Kadanwari-10.

Table 4.2 Petrophysical summary of well Kadanwari-10.

Parameters	G Sand	F Sand	E Sand
Depth (m)	3140-3251	3251-3323	3323-3351
Gross (m)	111	72.5	27.5
Net (m)	36.875	14.226	15.274
Net/Gross	33.2	19.6	55.5
Net Pay	36	12.851	15.274
V _{sh} (%)	15	19.4	11.5
Porosity (%)	21	14.4	28.2
S _w (%)	24	24	13.8
S _h (%)	76	76	86.2

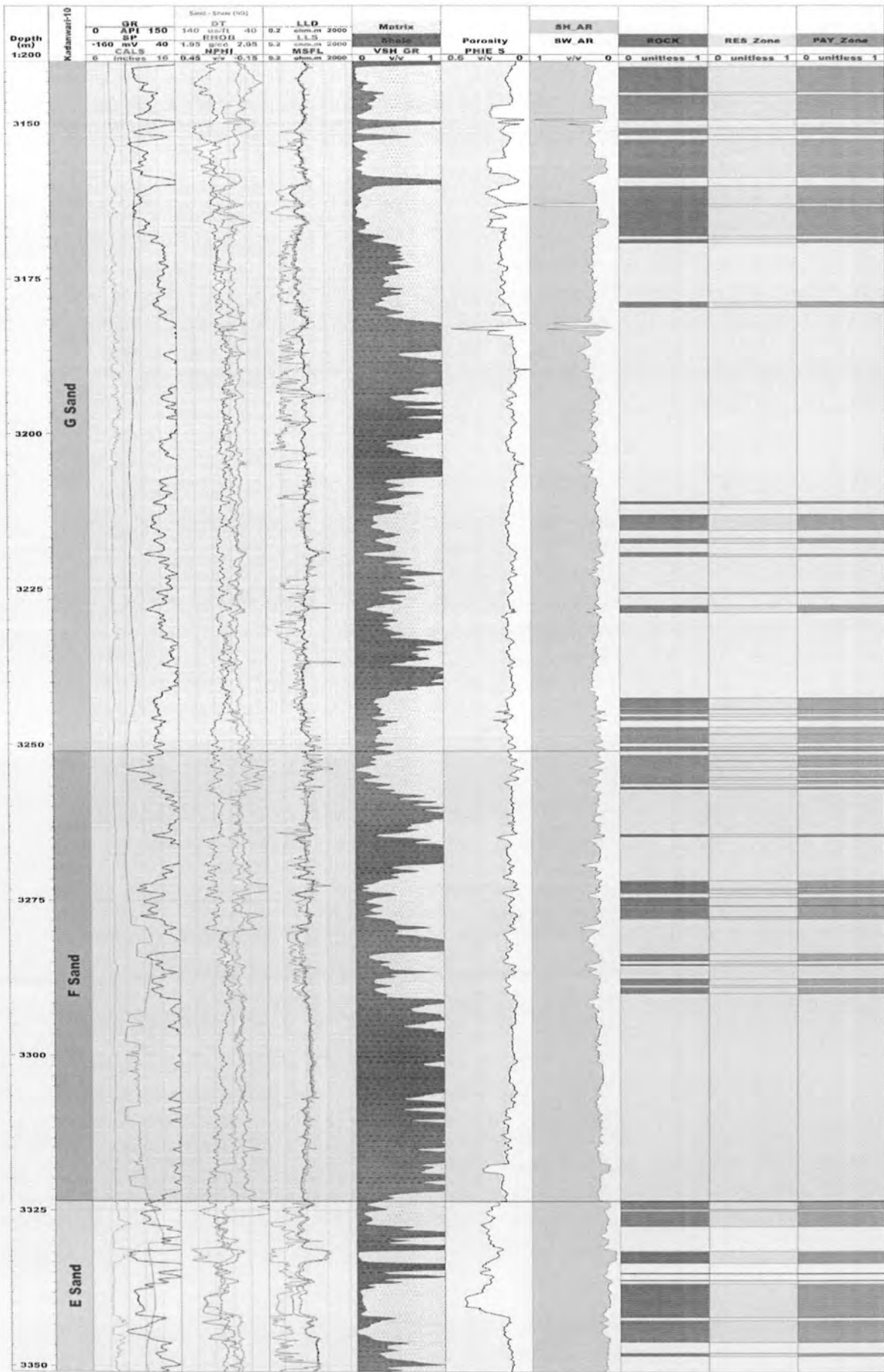


Figure 4.2: Petrophysical Analysis of well Kadanwari-10.

4.5 Facies Analysis

Accurate description of the fluids presents in the reservoir and its lithology is very important to minimize the risk factor in exploration of hydrocarbons. Facies analysis is done to use those rock properties that differentiate between fluid types and lithology of reservoir rocks. Basically, moduli such as elastic, shear, Bulk and lames constant is used for reservoir fluid and lithology discrimination. But some more parameter such as velocity of P-wave and S-wave, density, P and S-wave Impedance, V_p/V_s , Lambda-rho and Mu-rho are also used for characterization of reservoir.

4.5.1 LMR cross plot analysis

Cross plot between lambda-rho that is incompressibility modulus and mu-rho which is shear modulus is very helpful in differentiation fluids and lithologies of reservoir rock. Here density is plotted on z-axis to confirm the boundaries mark on the basis of lambda-rho and mu-rho values.

If $\lambda > \mu$, its means material has more incompressibility factor than rigidity and shape of the grains deformed by anisotropic stresses have large aspect ratios. Such grains are usually present in laminated shales. If $\lambda = \mu$ than grains have aspect ratio value 1 and this type of grain is mostly found in sand. So, we can differentiate easily between sand and shale on the basis of this cross plot. For fluid and gas identification, we have to check the lambda value because it is greatly affected due to their presence. The effect of Gas on incompressibility factor is greater than brine. Goodway (1999, 2001) and Dewar and Downton (2002) So we can identify the presence of gas by low value of lambda-rho with associated high value of mu-rho. In Figure (4.3) three zones are marked. Gas sand is marked by low value of lambda-rho and moderate to high value of mu-rho which is confirmed by low value of density due to gas presence, Brine sand is marked by slight greater value of lambda-rho than in gas sand. Shale zone is marked by high value of lambda-rho and low value of mu-rho with high density value.

4.5.2 Lambda-Rho Vs P-Impedance

Hydrocarbon zone have low value of lambda-rho and P-impedance. Sand and shale lithologies are marked by low and high value of Lambda-Rho respectively. Gas sand zone is marked by low value of lambda-rho and P-Impedance. Shale zone is marked by high value of lambda-rho. Density is used to confirm the discrimination done in this cross plot. Figure (4. 4) represents the cross plot between Lambda-Rho and P-impedance.

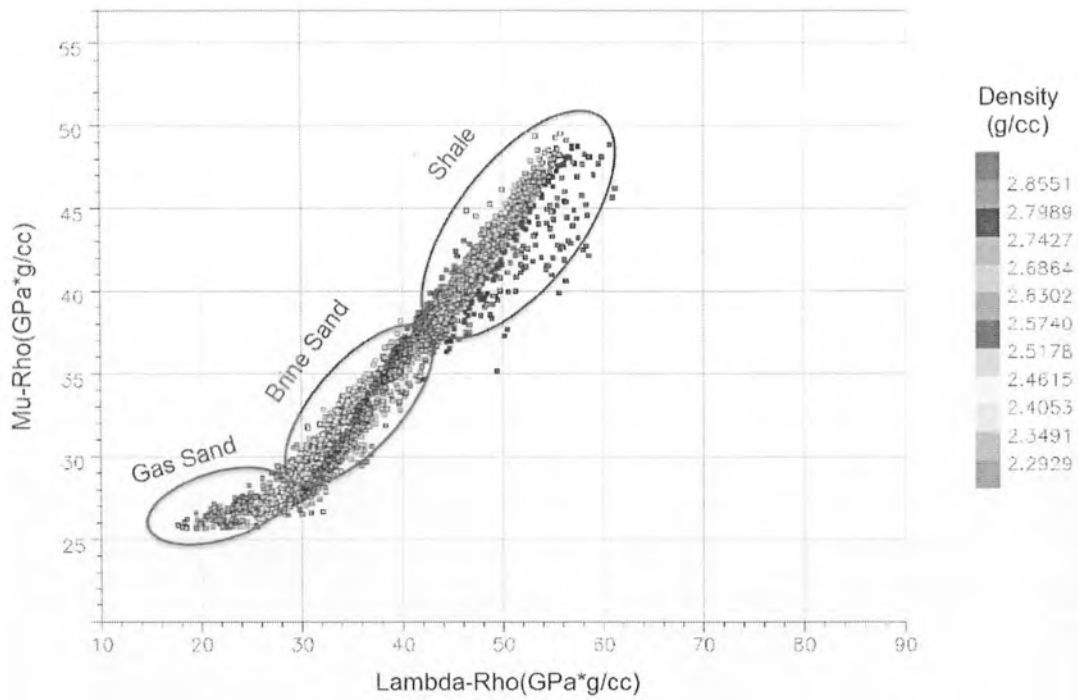


Figure 4.3: Lambda-Mu-Rho cross plot.

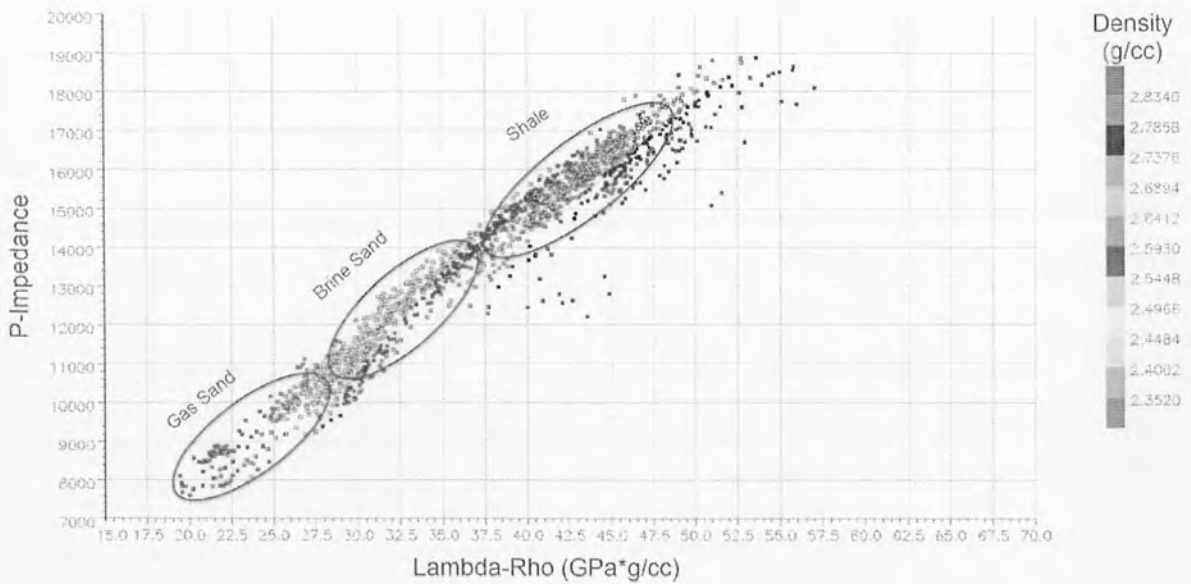


Figure 4.4: Cross plot between Lambda-Rho and P-Impedance.

4.5.3 Density Vs Poisson ratio

Gas saturated sand have low value of density than normal values and poisson ratio for gas saturated sand is usually upto 0.25. In this cross plot another parameters Lambda-Rho is used to confirm the zonation. Figure (4.5) shows the cross plot between density and poisson ratio in which Gas sand is marked on the basis of low value of PR and Density, while the shale is marked by higher value of density and corresponding PR value.

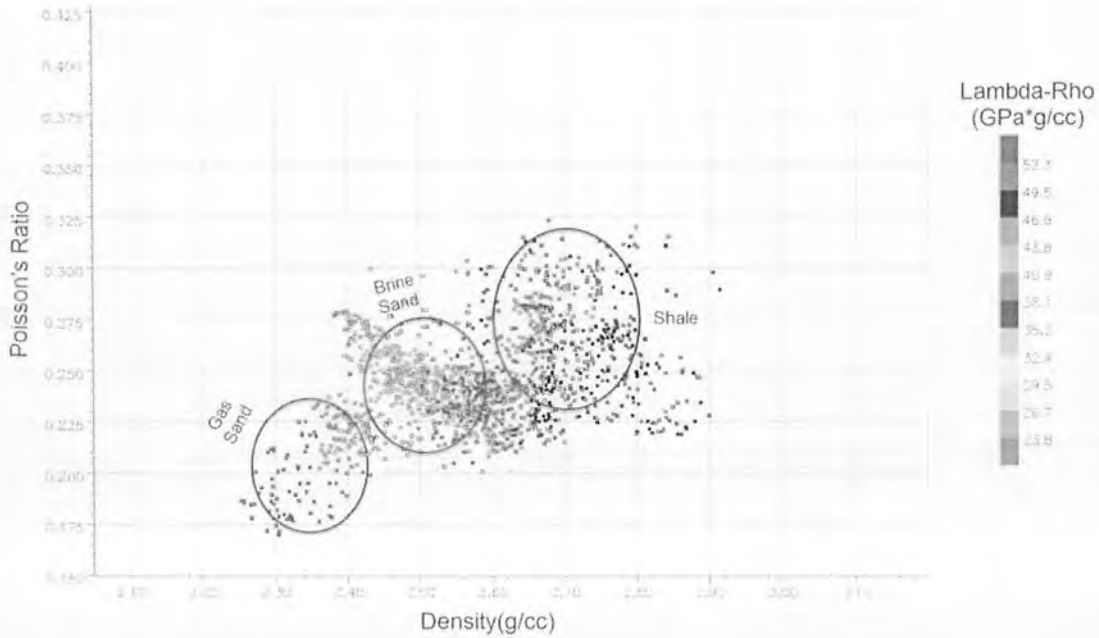


Figure 4.5: Density Vs Poisson ratio cross plot.

4.5.4 P-impedance Vs Vp/Vs

Hydrocarbon zone have low value of P-Impedance and Vp/Vs. P-wave velocity decrease and S-wave velocity increase due to increase in hydrocarbon saturation that's why Vp/Vs is very sensitive to change of fluids. Cross plot between these two parameters is very useful for differentiating the gas sand from brine sand and sands from shale lithology. In Figure (4.6) hydrocarbon bearing zone is identified on the basis of low P-impedance and low value of Vp/Vs. High P-impedance value indicate shale zone.

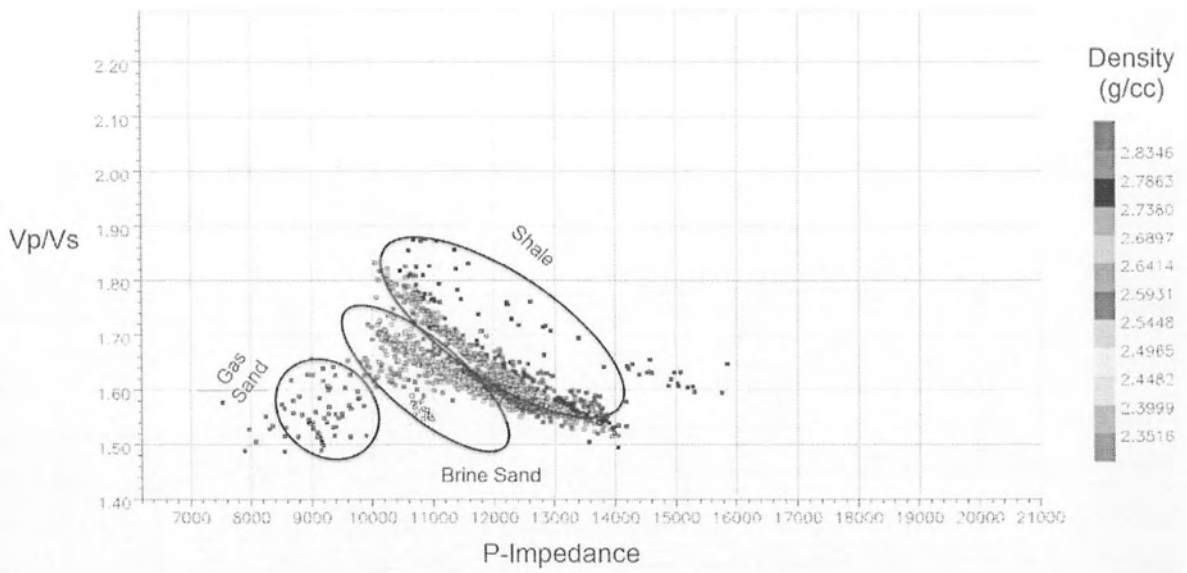


Figure 4.6: Cross plot between P-impedance and Vp/Vs.

CHAPTER # 5

FAULT SEAL AND SEISMIC ATTRIBUTE ANALYSIS

5.1 Fault Seal Analysis

5.1.1 Introduction

Mostly structural traps are associated with faults. These faults act as a seal or transmitter of the fluids flow. To recognize the fault behavior is very important for successful hydrocarbon drilling and exploration. Faults which are not acting as a seal allows the fluids to migrate from structures. In fault seal analysis two things are most important which are also related to each other's.

- Fault Architecture
- Fault rock properties

Fault architecture means size and shape of the fault, its orientation and inter-connectivity. Rock properties also affect the fault sealing capability. Local facies, type of fluids with in reservoir and their saturation level, pressure difference across faults, burial and fault history affect the properties of rocks.

5.1.2 Methodology

There are three main steps in fault seal analysis;

- Juxtaposition
- Fault zone deformation process
- Reactivation

In juxtaposition, we check the juxtaposition of foot wall and hanging wall lithologies along faults. If impermeable seal unit (shale) is present across the reservoir unit (sandstone) due to displacement along fault, then it is referred as juxtaposition seal.

Fault zone deformation process involves grain sliding and cataclasis, diagenesis of fault zone and clay smear. (Kaldi, 2008) Sometime juxtaposition seal is absent and sand on sand juxtaposition is present instead of sand across shale. In these cases fault itself is acting as barrier (seal) to hydrocarbon flow that is due to clay smear, diagenesis and cataclasis.

Clay smear give us idea that how much clay is incorporated into fault zone. If shale to sand ratio is greater than more clay is involved in fault zone. So, a method is used to predict the seal that is Shale Gouge Ratio (SGR).

Shale Gouge Ratio is defined as "Percentage of shaly material which slips past a point on fault". In this method, something's are very important such as:

- Clay bed thickness
- Number of clay beds
- Fault throw

If the bed of clay is thicker then more clay is present in fault zone. If the throw of fault is greater than abrasion smear is eroded and if the distance from source layer of clay is increased then thickness of shear smear is decrease.

Yielding et al., (1997) gives method to calculate the value of shale gouge ratio such as:

$$SGR = \frac{\sum \text{Shale bed thickness}}{\text{Fault throw}} \times 100\%$$

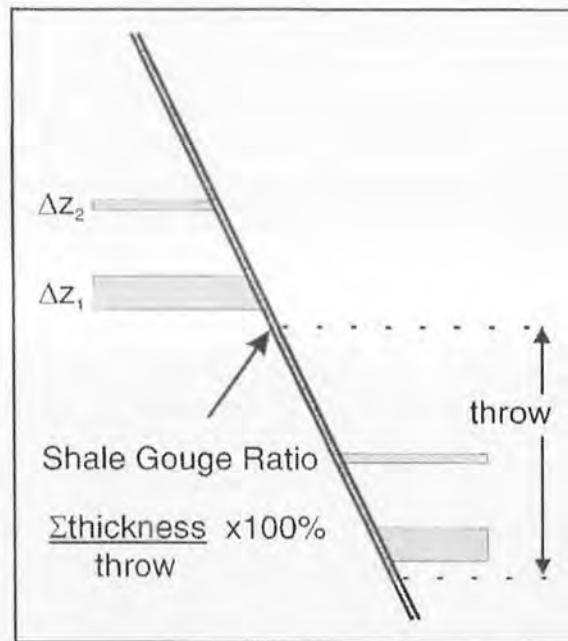


Figure 5.1: Shale gouge ratio method.

Diagenesis is a cementation along the fault plane which is permeable and removes the porosity and provides hydraulic seal. While cataclasis is the sand grain crushing which produce fine grained fault gouge material and provide high capillary entry pressure to fault.

5.1.3 Juxtaposition of the lithologies

Figure (5.2) shows the juxtaposition diagram to display the juxtaposition of shale and sand lithologies at fault location. Because some time seal is due to presence of different lithology across fault such as shale is present across sand which act as a seal to trap the hydrocarbons. It depends upon the throw of the faults. If the throw is greater than lithology thickness than we can find shale is present completely across the sand lithology and it's a good seal. But some time throw is smaller and lithologies are juxtaposed such as some

portion of sand is present across shale and some across sand. So in this case we check the Shale-Gouge ratio, whether fault itself act as a seal here or not. In Figure (5.2) good lithological juxtaposition is present at G sand level but at some places sand to sand juxtaposition is also present. As a whole juxtaposition seal in better at E sand level then at G sand depth.

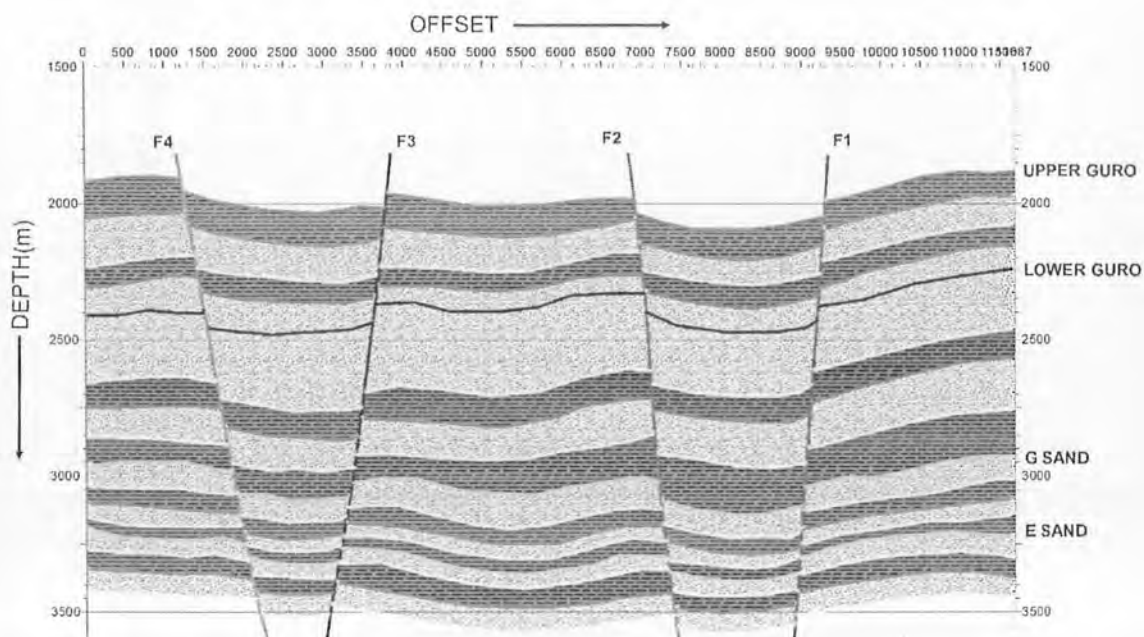


Figure 5.2: Juxtaposition diagram showing the Lithological juxtaposition.

5.1.4 Shale-Gouge Ratio

It's a percentage of shaly material that slips due to fault. So, SGR value for Red fault is 20 percent at E Sand level because throw of fault is up to 50 m there. While at G Sand level SGR value is up to 70% and here throw is up to 60m. If SGR is between >18% it indicates high possibility of seal. SGR value of Light blue fault is less than sealing capability.

5.1.5 Conclusion

By juxtaposition diagram and SGR value, it is clear that the Fault F1 which is displayed with red colour is acting as a seal, because we are getting good juxtaposition seal at reservoir depth along this fault and fault gouge ratio is also high that indicating the sealing capability of fault. Along this fault Kadanwari-10 well is drilled.

5.2 Seismic Attribute Analysis

These are measurements which based on seismic data such as frequency, phase and polarity. Geoscientist uses these attributes as quality control in characterization of reservoir. They are used for quantitative as well as qualitative measurements such as horizon and fault, dip etc. They reveal such information which cannot be extracted from seismic amplitude data. They give us information about the shape of seismic waveform, its position and amplitude. They are used to identify the prospect zone, certain environments of deposition, faults and fracture pattern for structural study of that area and use as direct hydrocarbon indicator. (Koson et al., 2014) Amplitude is the default seismic attribute, which is very important for finding the reflection coefficient, absorption etc. Phase is used to find the reflectors shape and geometry. These are divided into two categories.

Physical attributes which are related to lithology and wave propagation and geometrical attributes which are related to dip of the reflectors, discontinuity pattern etc.

5.2.1: Reflection Strength Attribute (*Envelop of trace/Instantaneous Amplitude*)

Reflection strength is related to the reflection means acoustic impedance contrasts. It results strong acoustic events on positive and negative events. It is independent of seismic data polarity and phase. It is proportional to the reflection coefficient magnitude and shows the instantaneous energy.

This attribute is mainly useful in identifying:

- Bright spots.
- Lithology change
- Faults
- Tuning effect
- Sequence boundaries
- Depositional environments.
- Unconformities.

Figure (5.3) shows the results of Reflection strength attribute applied on seismic line TJ89-512. It shows the discontinuity in the layers which is confirming the interpretation already done on section of seismic line TJ89-512. Thick packages in this section represent the full reflection strength which is probably source, reservoir and seal zones.

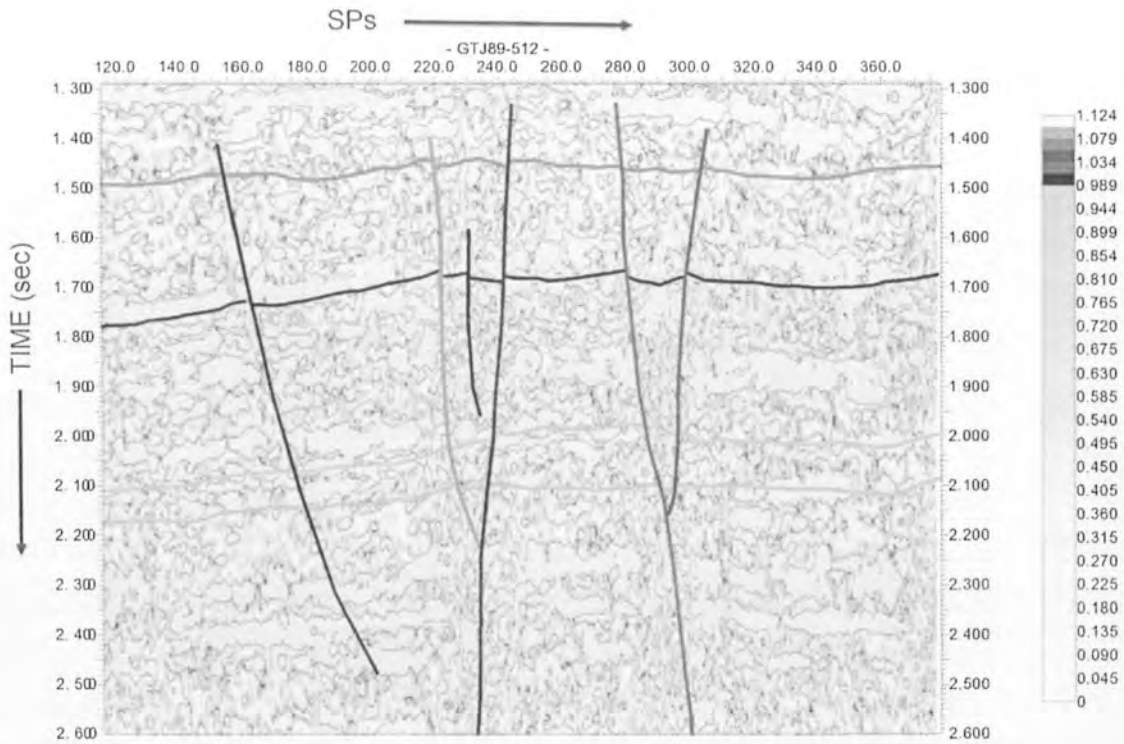


Figure 5.3: Reflection strength attribute applied on TJ89-512.

5.2.2 Instantaneous Phase

It displays the events both weak and strong with equal strength. It is independent of amplitude and very useful for discrimination of geometrical shapes and to check the lateral continuity of reflectors. It can be computed from real and imaginary seismic traces using a mathematical relation given by Taner et al (1977 and 1979).

$$p(t) = \tan^{-1}[q(t)/r(t)]$$

Where $q(t)$ is the quadrant seismic trace, and $r(t)$ is the real seismic trace.

This attribute is mainly useful in identifying:

- Lateral continuity of Horizons
- Unconformities and faults
- Pinch outs
- Angularities
- Patterns of sedimentary layers
- Compute phase velocity
- Compute instantaneous frequency and acceleration
- Detailed visualization of stratigraphic elements

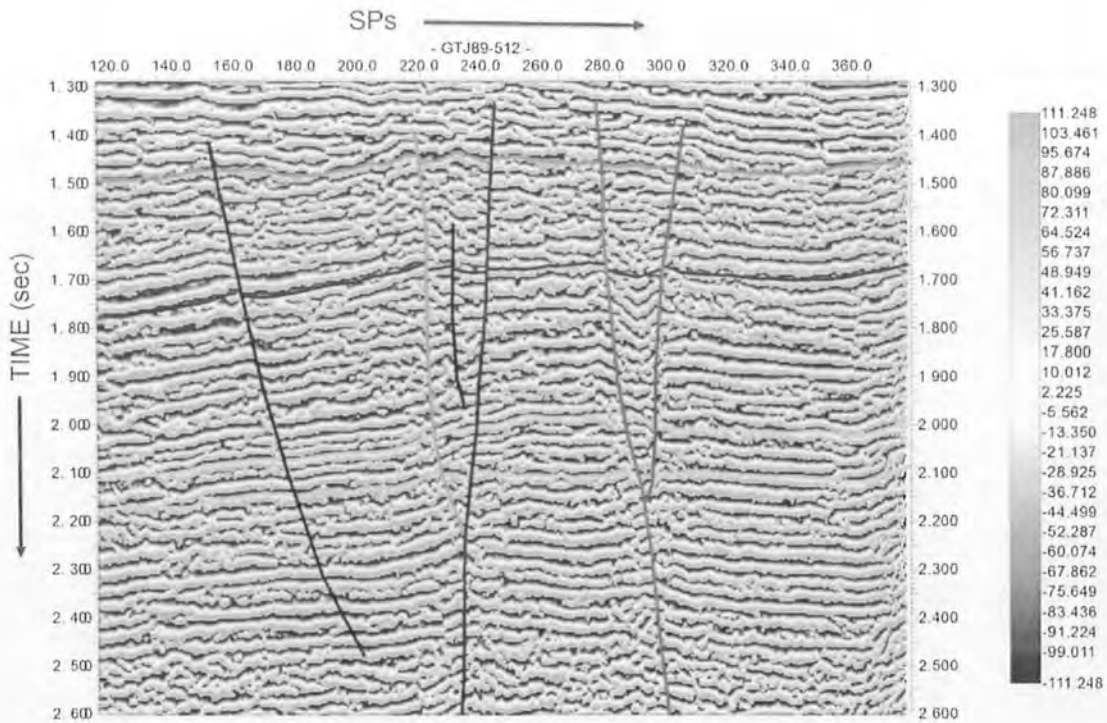


Figure 5.4: Instantaneous phase attribute applied on seismic line TJ89-512.

Figure (5.4) shows the instantaneous phase attribute applied on seismic line TJ89-512. The horizons marked on the sections are lies over the zero phase regions. So, attribute confirms the interpretation as the input data is zero phase.

5.2.3 Average energy

In this attribute, the square root of the sum of squared amplitudes is calculated for a specific window and then divides it by the total number of samples. It shows the average value for each cycle and its appearance is blocky. It gives the spatial variation in the wavelet response. Negative value in the colour bar indicating trough region of the seismic trace.

This attribute is mainly useful in identifying

- Lithological variation
- Stratigraphic variations
- Direct hydrocarbon indicator

Figure (5.5) shows the seismic line TJ89-512 over which average energy attribute is applied.

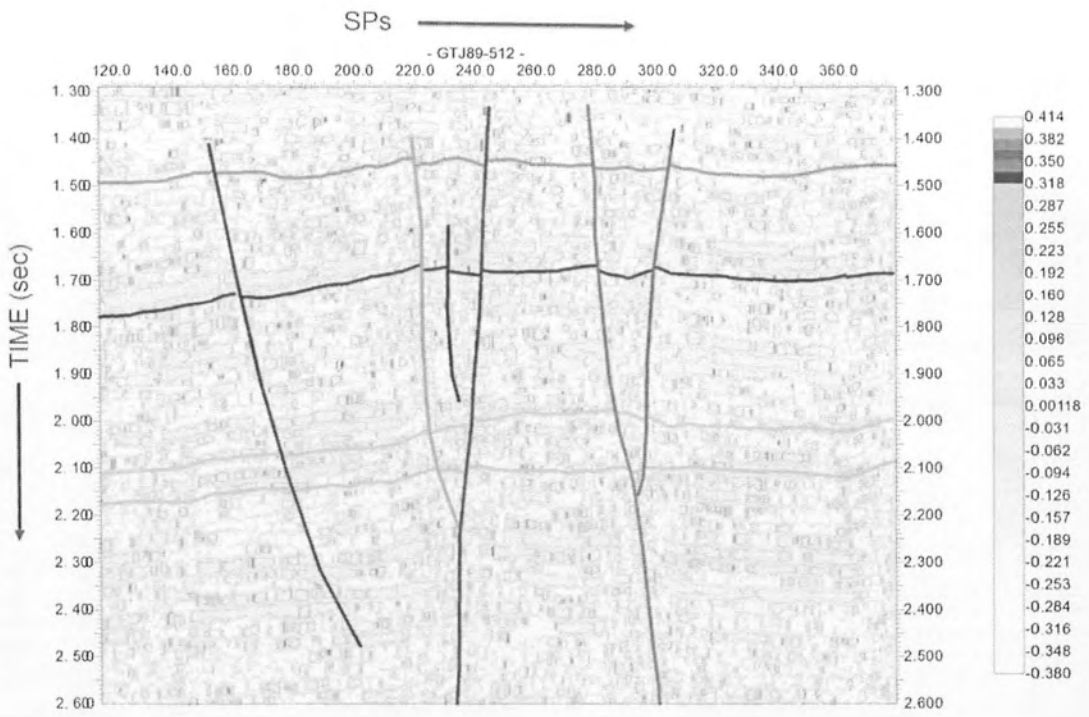


Figure 5.5: Average energy attribute applied on seismic line TJ89-512.

CHAPTER # 6

SEISMIC INVERSION

6.1 Introduction

Inversion is the inverse of forward modeling. In forward modeling, we start with earth properties model and by applying physical processes such as acoustic we get the final output model. While in seismic inversion we start from measured data and apply the process to get back the earth model. (Barclay et al) In this method we transform the amplitude values to the impedance values.

There are two types of seismic inversion.

- Post stack inversion
- Pre-stack inversion

In this project post stack inversion is applied. In post stack inversion, we use seismic data and well data to change the seismic data into acoustic impedance. Acoustic impedance is the product of density and velocity. In this the main parameters are impedance values, density, P-wave velocity and S-wave velocity but we can predict reservoir properties such as porosity, lambda-rho (Incompressibility factor), shear modulus (μ), poisson ratio, net-to-gross, lithology, pore pressure and saturation etc. (Saxena et al., 2008)

6.2 Methodology

Different techniques have been used for post stack inversion. Such as:

- Model based inversion
- Sparse spike inversion
- Band limited inversion
- Coloured inversion

6.2.1 Model Based Inversion

It starts with initial layer model whose depth and thickness is known and velocities and density values are derived from well data. This model has velocity and density values which are further used for inversion to get impedance values. If model have P-wave velocities than we get the acoustic impedance and if it contains shear velocities than shear impedance can be obtained. Model is convolved with wavelet to get synthetic trace. This synthetic trace is compared with actual seismic trace and find out the difference between both traces. This difference is used to modify model so synthetic trace become closely resemble to actual seismic trace. It's not a one step process, it remains continue with generation of different models by making iteration to minimize the difference between the real seismic trace and the synthetic trace until the model is obtained which is best fit. (Barclay et al) Figure (6.1) shows the work flow of model based inversion.



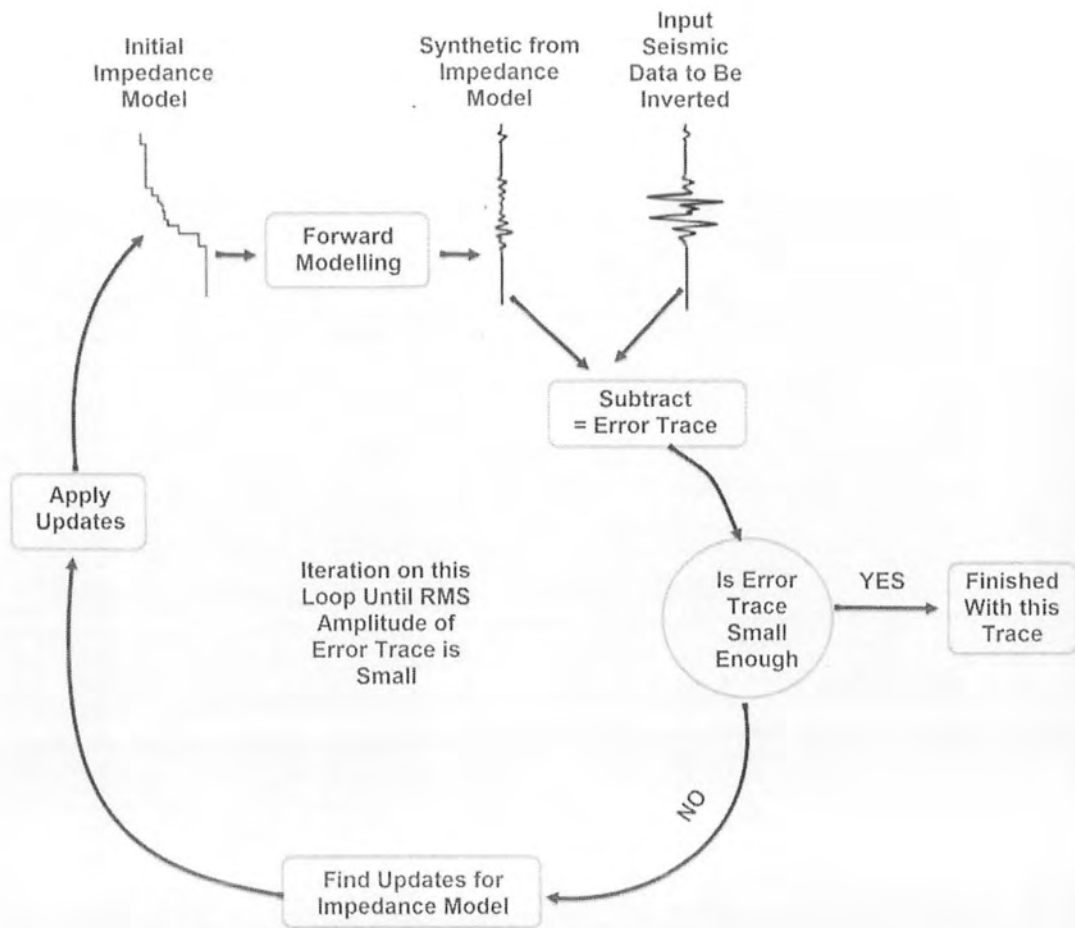


Figure 6.1: Model Based Inversion work flow.

The main approach is to minimize this function: (Russell and Hampson, 1991)

$$J = weight_1 X (T - W * r) + weight_2 (M - H * r)$$

Where

T= Seismic trace

W= Wavelet

r = Final reflectivity

M= Initial model

H= Integration operator model.

Minimization of the first part gives a solution which model the seismic trace and second gives the initial impedance model.

The main thing in this method is initial model which gives reservoir geometry. Parameters which are required for this are horizons and well data. Figure (6.2) shows the initial impedance model which is generated using well data of Kadanwari-10 and seismic horizon extracted from 3D seismic data.

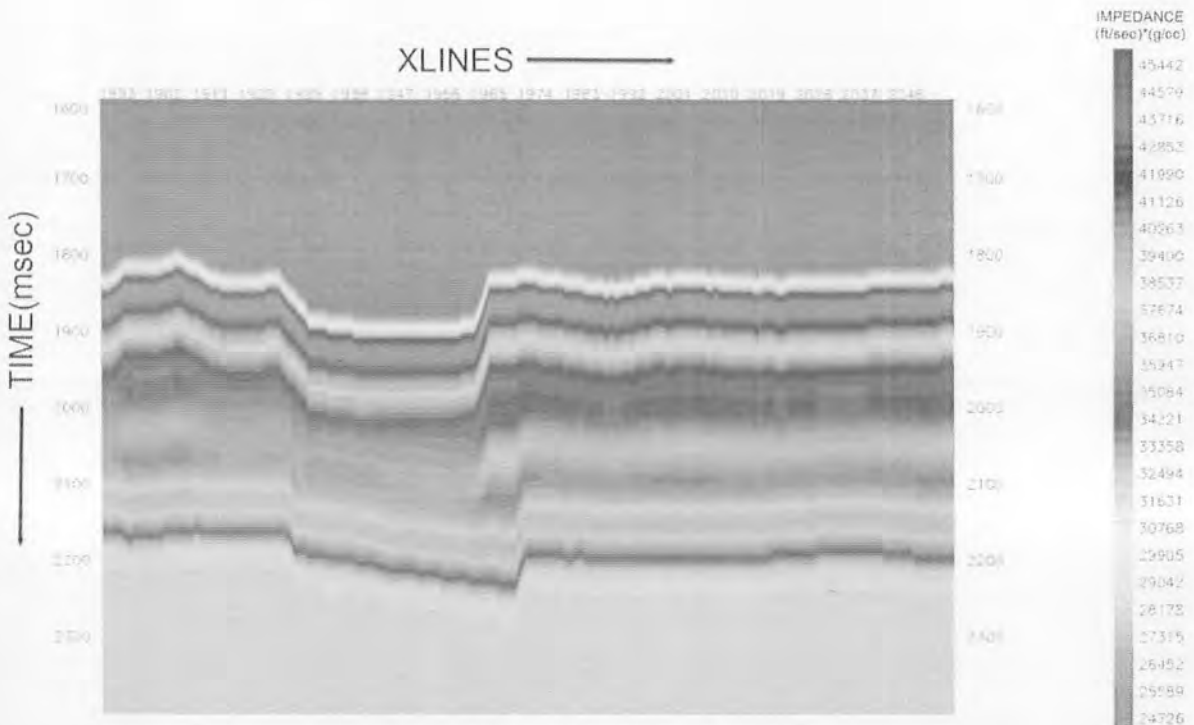


Figure 6.2: Initial impedance model.

6.2.2 Inversion Analysis

Figure (6.3) shows the inversion analysis at the location of the well Kadanwari-10. Red colour log shows the inverted result and blue represent the original data while black log is the initial model. Red traces are synthetic traces while black traces are seismic traces. Time window selected is from 1800msec to 2200msec. Correlation factor between inverted and original data is 0.996 while error between them is 0.087.

Inverted seismic section of Inline 2004 is shown in Figure (6.4). Higher impedance values represent the shaly units while the low impedance represents the sand. G sand horizon is displayed at time 2000msec. At well point we are getting the low impedance values at G sand depth that are indicating the presence of gas.

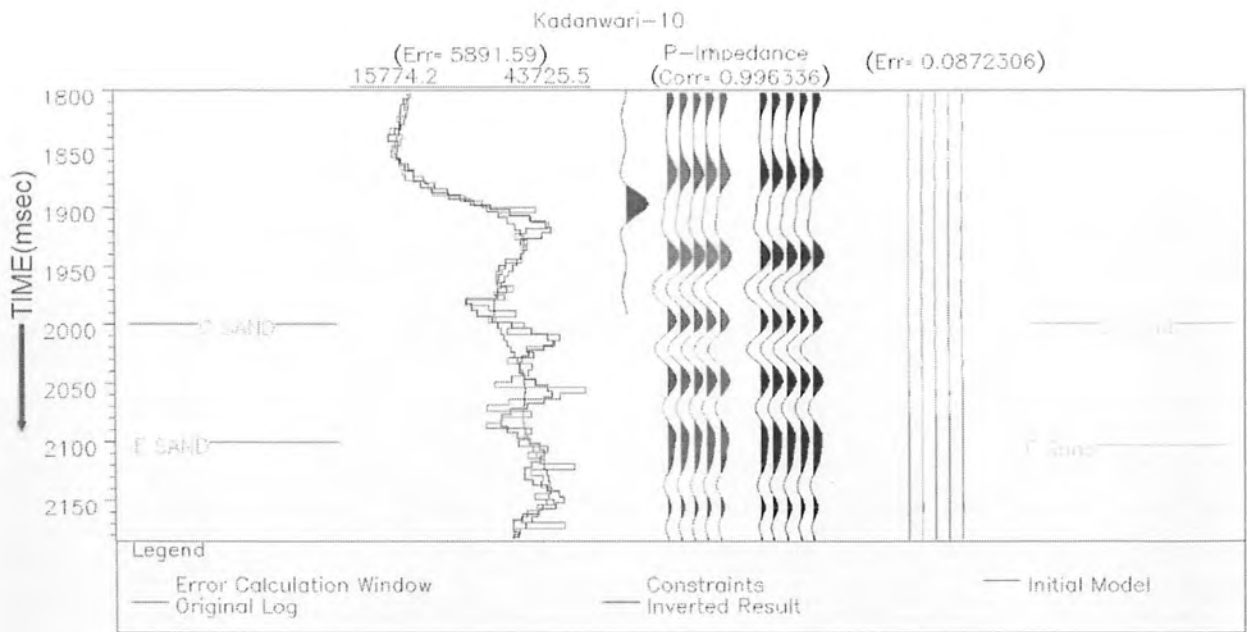


Figure 6.3: Inversion analysis at well Kadanwari-10.

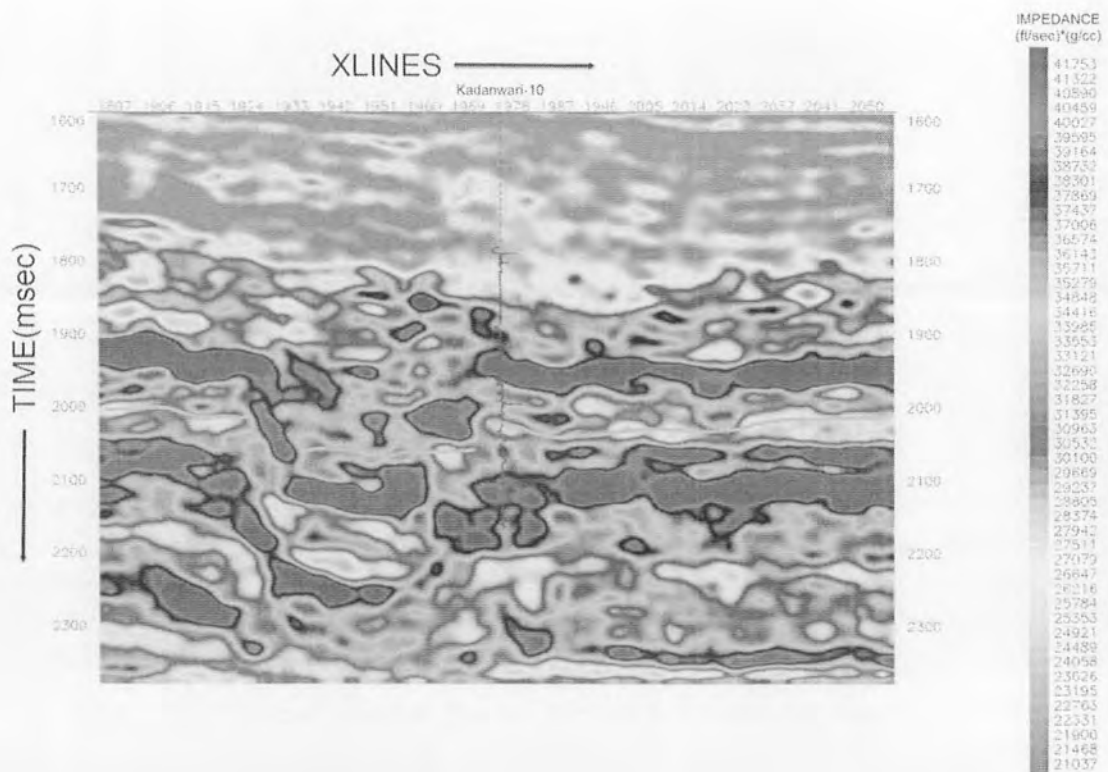


Figure 6.4: Inverted section of Inline 2004.

6.3 Density Section

Density is very important and helpful property to define the lithologies. Figure (6.5) shows the inverted density section of inline 2004. At time 2000msec value of density is varying from 2.25 to 2.35g/cc which is a sand body and marked as G sand. At well point density of sand is too low which is the indication of gas presence. While above the G sand there is a package with purple colour having high density values is shaly unit.

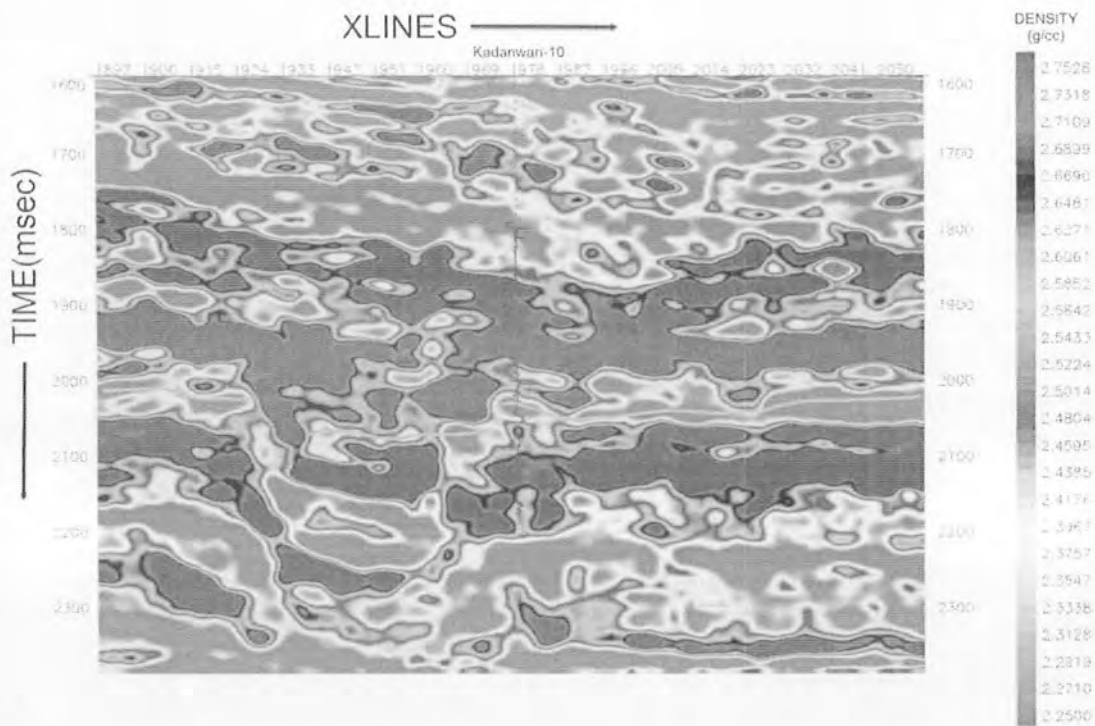


Figure 6.5: Inverted Density section of seismic inline 2004.

Figure (6.6) shows the density distribution map of G Sand in this area. At well point density value is low due to presence of gas. At some points, we are getting high density values which are due to shale.

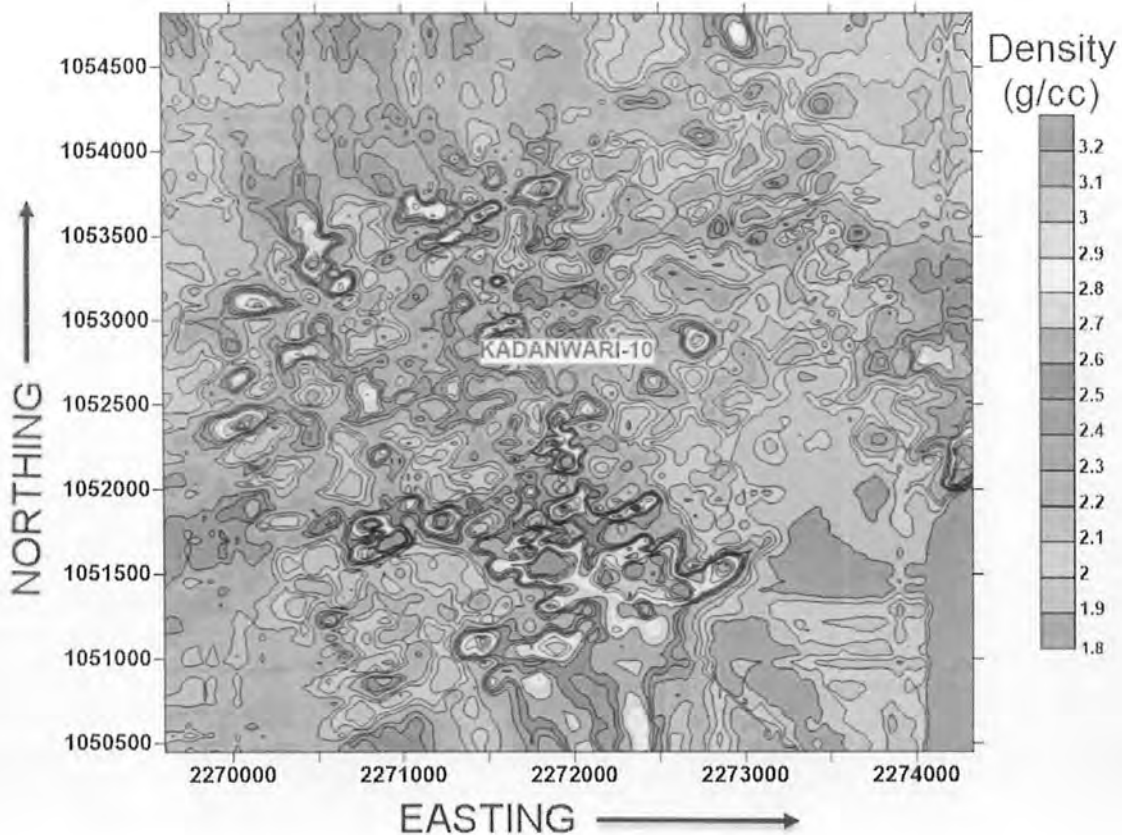


Figure 6.6: Density distribution map of G Sand.

6.4 Porosity calculation

Porosity calculated from by seismic inversion improves the reservoir characterization. It provides information about the spatial variation in the porosity values away from the well point. Vertical resolution of seismic maps is in tens of meters. So, the porosity generated by this have the effect of averaging vertically, reducing variation in porosity which is very important for reservoir characterization. They are also used for volumetric estimation and sweet spot identification. Before predicting the porosity, we must have understanding that how the seismic response is affected by fluids and rocks changes.

A linear relationship was generated between the acoustic impedance and the porosity using the well data of Kadanwari-10.

$$Porosity = m * acoustic\ impedance + c$$

Where m is the slope and c is the intercept value. Figure (6.7) shows the plot between acoustic impedance and porosity of well data Kadanwari-10.

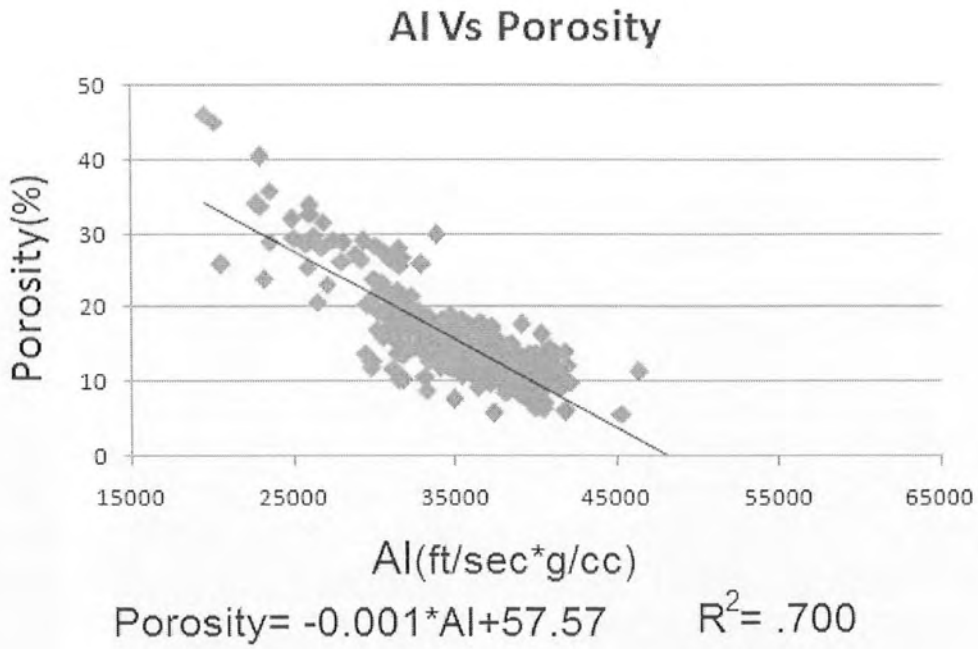


Figure 6.7: Cross plot between Acoustic Impedance and Porosity.

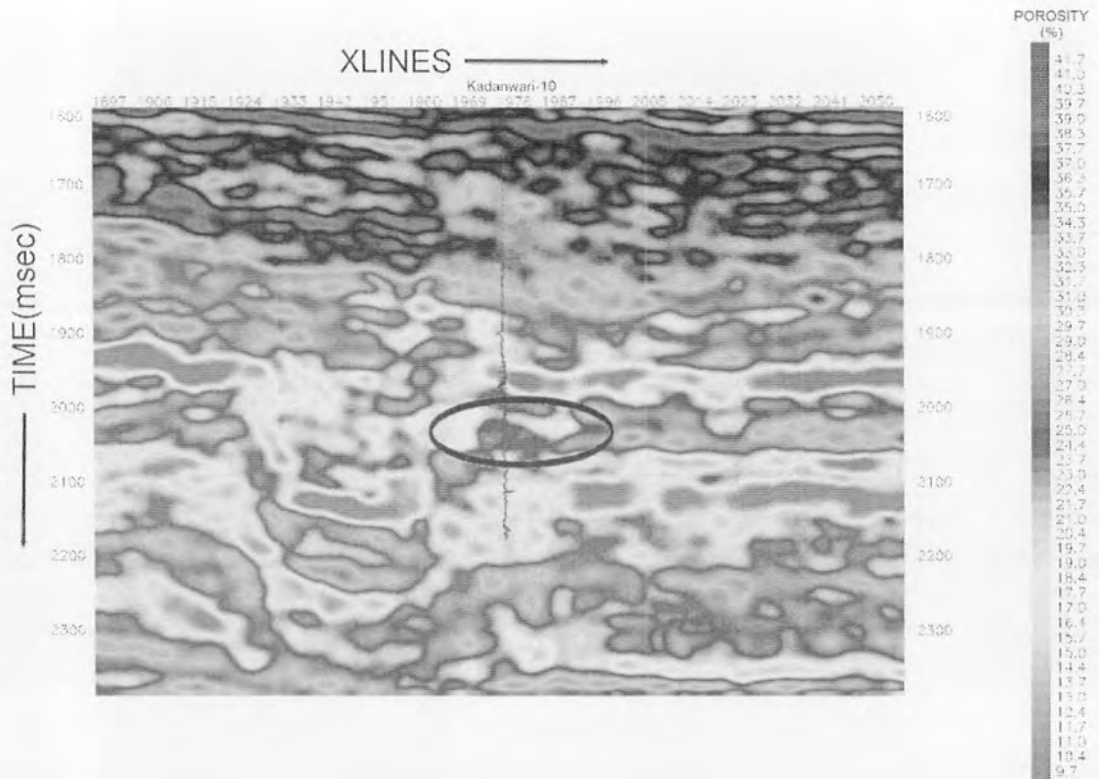


Figure 6.8: Porosity section of Inline 2004

Figure (6.8) shows the porosity section of seismic Inline 2004. At time 2000msec a layer is present having porosity value ranging from 17 to 32 percent which is G sand. At well location porosity value is about 23% which is confirming the petrophysical analysis of G sand. Layer above G sand having low value of porosity is shaly unit.

Figure (6.9) shows the porosity distribution map of G Sand within area over which 3D seismic data is available. Mostly porosity values lie between 16 to 3%. In south-eastern part G Sand have very good porosity between 30 to 42%. Kadanwari-10 well is displayed in this map, at well location porosity value is about 23% which is similar to petrophysical result of well Kadanwari-10.

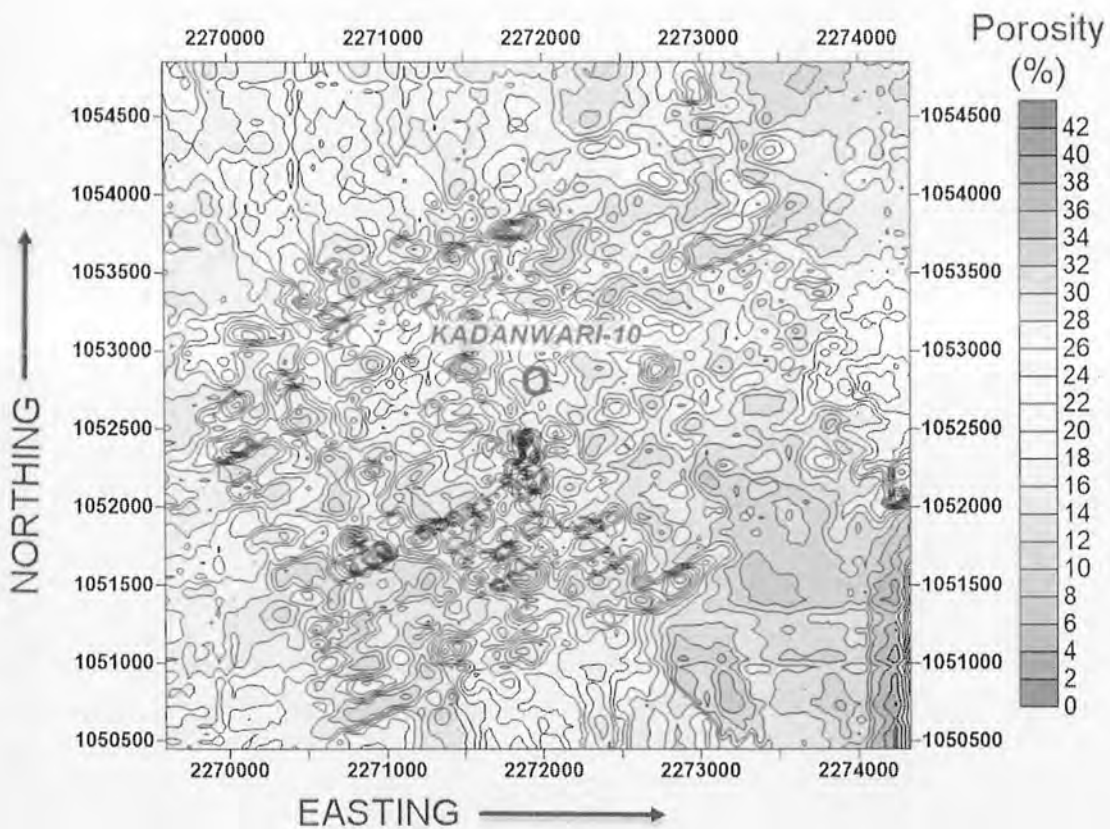


Figure 6.9: Porosity distribution map of G Sand.

6.5 Lambda-Mu-Rho calculation

LMR method is proposed by Goodway et al.(1997) to identify the gas sands. It utilize Lamé's parameters (λ and μ) and density. (Russell and Hampson, 1991)

Lamé's parameter can be calculated as:

$$\mu\rho = SI^2$$

$$\lambda\rho = AI^2 - 2SI^2$$

Where AI is acoustic impedance, SI is shear impedance and ρ is the density. In this Lambda-Rho gives fluid value and Mu-Rho gives the rock matrix value.

Lambda is the incompressibility factor, which will be decrease if the fluid is present in the rock. But the effect of gas on Lambda is greater than presence of brine in the rock. So the value of Lambda is more decreased if gas is present in the rock. This method is also helpful to identify the sand versus shale lithologies. If the value of Lambda is greater than Mu then it indicates shale lithology because in this case grains have large aspect ratio which is usually present in shale. If both are equal, than it indicates sand lithology because aspect ratio become 1 and this behavior is present in sand grains.

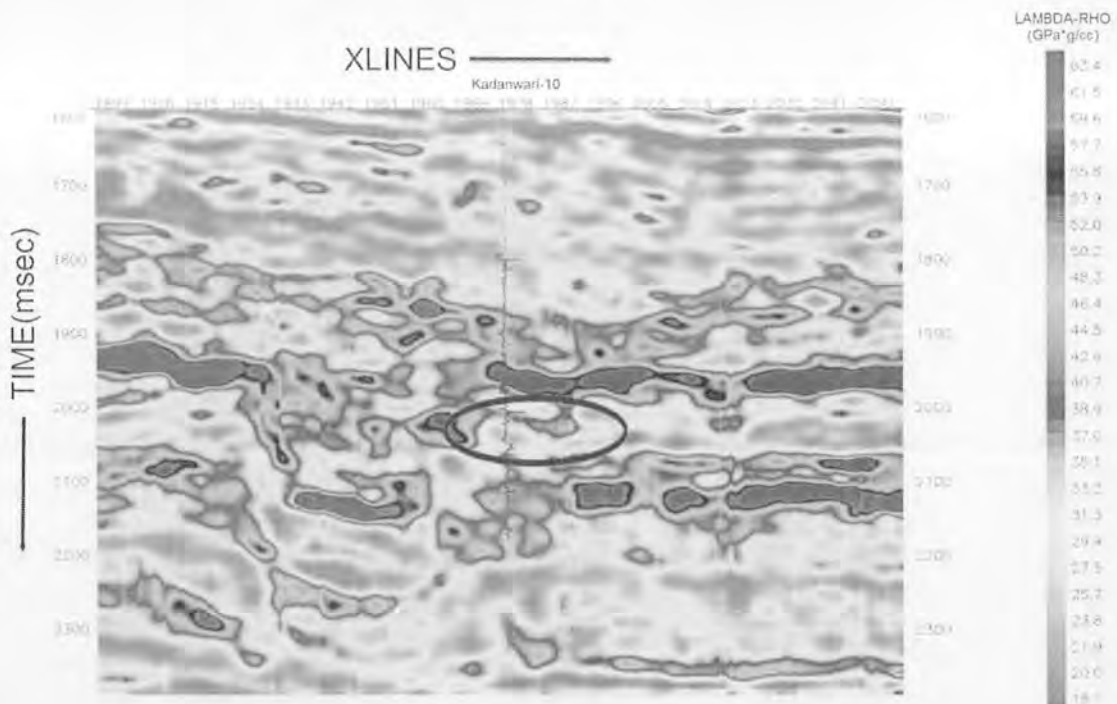


Figure 6.10: Lambda-Rho section of seismic Inline 2004.

Figure (6.10) show the Lambda-Rho section of seismic inline 2004. At time 2000 msec there is a zone which has low value of Lambda-Rho that is the G sand which is gas sand in the well Kadanwari-10.

Figure (6.11) shows the Mu-Rho section of seismic inline 2004. At well point of Kadanwari-10 we are getting value of Mu-Rho greater than Lambda-Rho which indicates the presence of gas at G sand depth.

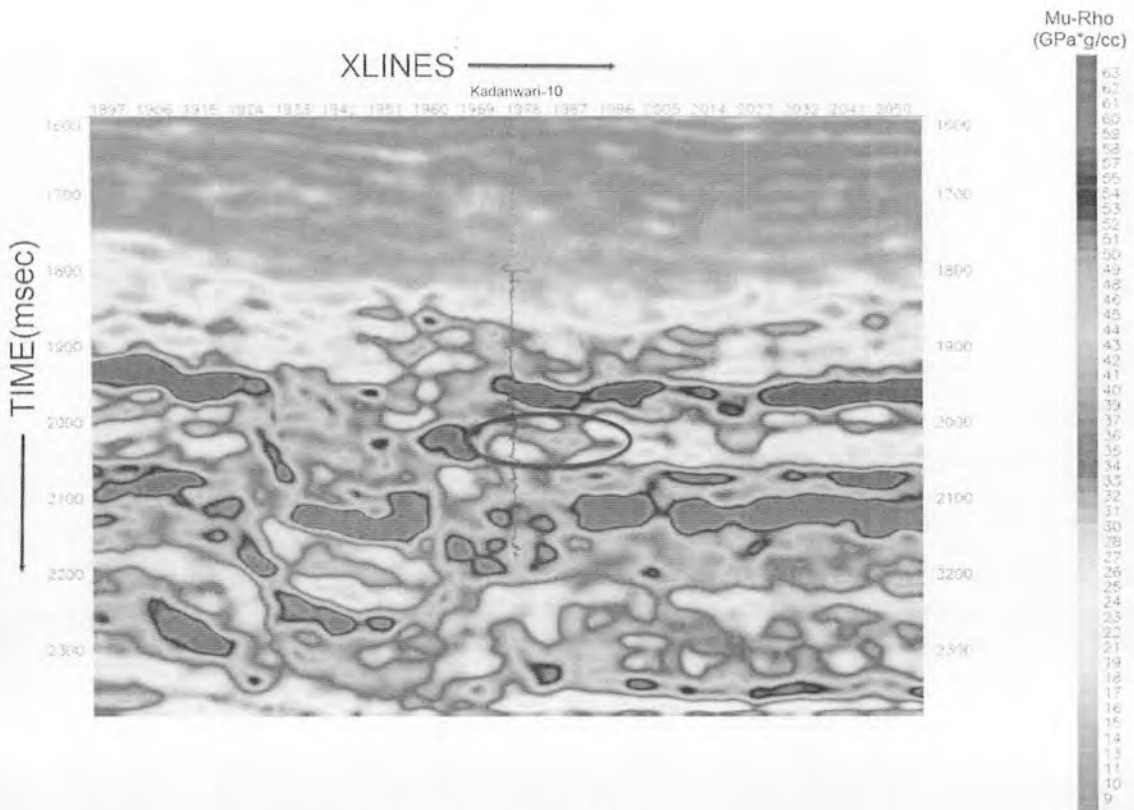


Figure 6.11: Mu-Rho section of seismic inline 2004.

6.6 Vp/Vs calculation

Vp/Vs is widely used to identify the fluid types and differentiate the gas zone from water. Because P-wave velocity becomes decreased due to hydrocarbon saturation and S-wave velocity become increased. In gas zone Vp/Vs is mostly lies between 1.58 to 1.6. Figure (6.12) shows the Vp/Vs section of seismic inline 2004. Gas zone is marked on the section based on low ratio value which is G sand.

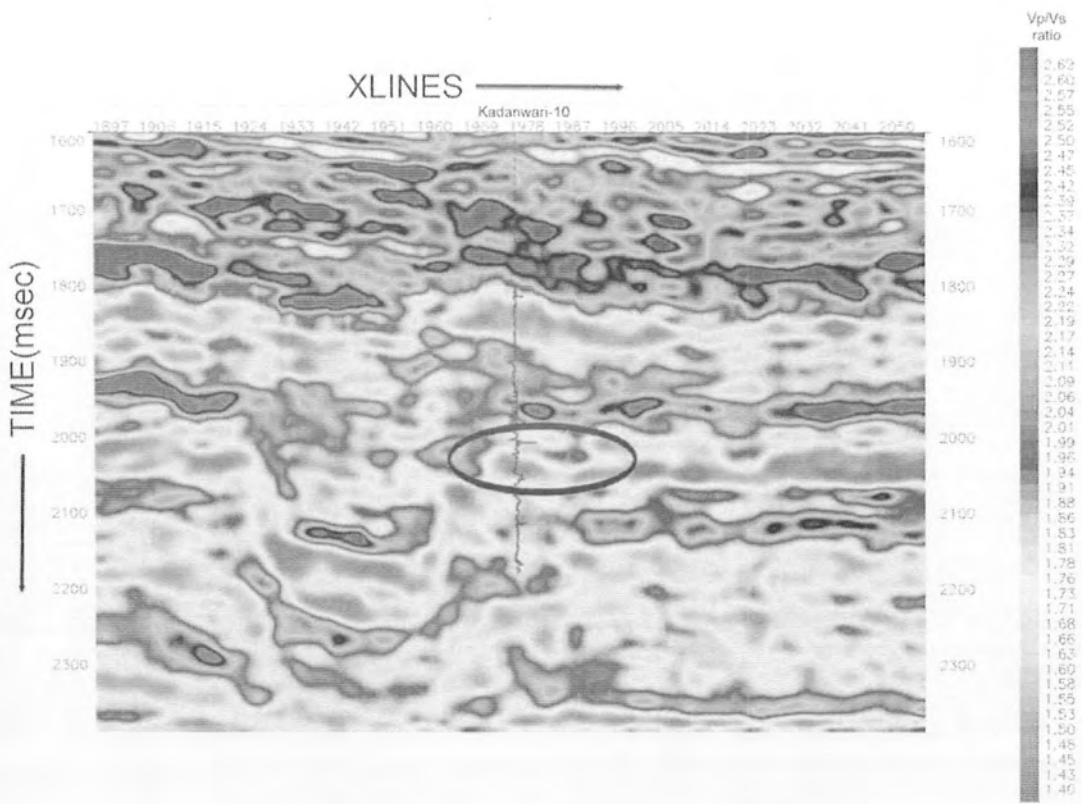


Figure 6.12: Vp/Vs section of seismic inline 2004.

CONCLUSION

- By using the well data and general stratigraphy of the area four horizons are marked on seismic sections along with faults.
- Seismic interpretation reveal that the structure in this area consist of normal faults. These faults are in the form of Horst and Graben.
- Main producing reservoir zones in this area are G and E sand but F Sand is also producing in some areas. Shale of Lower Goru and Upper Goru are acting as seal in the area and source rock is the Sember Formation.
- Petrophysical analysis of Kadanwari-08 shows that at the location of this well sands of Lower Goru have good porosity but they are mostly water saturated. Petrophysical analysis of Kadanwari-10 shows that G and E Sand of Lower Goru have which high hydrocarbon potential. In Kadanwari-10, G Sand have porosity value 21% with volume of shale up to 15% and 76% hydrocarbon saturation.
- Fault seal analysis is very helpful for identifying whether the fault is acting as a seal are not. Results of this analysis shows that the fault F1 present on the maps have a good sealing capability and along this fault Kadanwari-10 well is drilled which is gas producing well.
- Seismic inversion is very helpful for reservoir characterization. Reservoir zone is picked by low value of impedance on seismic inverted section. To confirm this reservoir zones other parameters are used such as Lambda-Rho, Mu-Rho and Vp/Vs and their section are generated using inverted impedance data. At reservoir zone which is G Sand zone, we get low value of Lambda-Rho with corresponding high value of Mu-Rho and low value of Vp/Vs.

REFERENCES

- Barclay F et al. Seismic inversion: Reading between the lines
- Berger et al., 2009, Porosity-preserving chlorite cements in shallow-marine volcanoclastic sandstones: Evidence from Cretaceous sandstones of the Sawan gas field, Pakistan, American Association of Petroleum Geologists (AAPG)
- Castagna, J.P., Batzle, M.L., and Eastwood, R.L., 1985. Relationships between compressional-wave and shear-wave velocities in clastic silicate rocks. *Geophysics*, V.50, pp. 571-581
- Dewar J., Downton J. 2002. Getting unlost and staying found – a practical framework for interpreting elastic parameters. Expanded Abstract CSEG Annual Conference 2002.
- Dix, C. H., 1955, Seismic velocities for surface measurements, *Geophysics*, Vol 20, pp. 68-86.
- Goodway W., Chen T., and Downton J., 1999. Rock parameterization & AVO fluid detection using Lamé petrophysical factors; λ , μ and $\lambda\rho$, $\mu\rho$. 61st EAEG meeting, Expanded Abstracts, 6-51.
- Goodway W. 2001. AVO and Lamé' constants for rock parameterization and fluid detection. *Recorder*, 26, 39-60.
- Kadri I.B., (1995), *Petroleum Geology of Pakistan*, PPL, Karachi, Pakistan.
- Kaldi, J., 2008, Evaluating reservoir quality, seal potential and net pay: Geo India pre-conference training.
- Kazmi, A.H., and Jan, M.Q., 1997, *Geology and Tectonics of Pakistan*, Graphic Publishers Karachi, Pakistan
- Koson et al., 2014. Seismic attributes and seismic geomorphology. Vol. 6, No. 1, 1-9
- Majid et al., 2016, Interpreting seismic profiles in terms of structure and stratigraphy with implications for hydrocarbons accumulation, an Example from Lower Indus Basin Pakistan, *J Geol Geophys*
- Mcquillin et al., 1984, An introduction to seismic interpretation , reflection seismic in petroleum exploration

Nasir et al., Porosity prediction using 3D seismic inversion, Kadanwari Gas Field, Pakistan. Pakistan journal of hydrocarbon research, Vol.17, (June 2007), p.95-102

Raza, H. A., Ahmed, R., Ali, S.M., Shaikh, A. M. and Shafique, N. A., 1989, "Exploration performance in sedimentary zones of Pakistan", Pakistan Journal of Hydrocarbon Research, v. 1, No. 1, P. 1-7.

Russell, B., & Toksöz, M. N. (1991, November). Comparison of post stack seismic inversion methods. In 1991 SEG Annual Meeting.

Saxena et al., 2008. Use of various amplitude inversion techniques for seismic reservoir characterization. P-439

Taner, M.T., and Koehler, F., 1979. Velocity spectra – digital computer derivation and applications of velocity functions, Geophysics, Vol.34, pp.859-881.

Wajid et Al., 2015, Evaluation of Petrophysical Properties for Reservoir Characterization of Eocene Age in Meyal Field, Potwar Basin-Pakistan ,Sci.Int.(Lahore),27(5),4187-4190,2015

Yielding, G., B. Freeman, and D.T. Needham, 1997, Quantitative fault seal prediction: AAPG Bulletin, v. 81, p. 897-917